Dear Dr. Shepson,

We have incorporated all of the comments and suggestions from Reviewer 1 and Reviewer 2 into this updated version of the manuscript. In particular, we have added a paragraph in the introduction that summarizes the atmospheric nitrogen measurements made during the UBWOS campaigns. We have also shortened the manuscript considerably by reducing repetition and combining several figures.

In the supplemental material we have added a figure showing snow nitrite measurements as well as NOAA HYSPLIT back trajectories for 12 days during the UBWOS2014 campaign. Snow nitrite concentrations are presented to provide a comparison of the magnitudes of snow nitrate to snow nitrite concentrations. Back trajectories are shown to provide insight into how the origin and path of boundary layer air masses in the Uintah Basin changed during the campaign.

Thank you for considering this manuscript for publication.

Sincerely,

Maria Zatko

Author response to Reviewer 1:

We thank Reviewer 1 for their thoughtful comments and suggestions.

General Comments:

The paper is too long and could be reduced by about 1/3 without any loss of and significant content.
We have shortened the manuscript by roughly 3 pages total by reducing repetition. Most of the reductions are in the results and conclusions sections, but we have made the introduction and methods section more concise as well. A novel approach is used in this study to assess photochemistry in mid-latitude regions. Since this approach relies heavily on both optical and chemical models and measurements, and is the first of its kind, we feel that it is appropriate to include thorough descriptions of the approach. We leave it to the editor to decide if we should shorten further by reducing content.

The measurements presented here lack context. For example we are not given any summary of what the level of total odd-nitrogen (NOy) was [Wild et al., 2016], we were not told of the presence of high levels of peroxynitric acid [Veres et al., 2015], nor N2O5, nor ClNO2, all species that might have significant impact on snow pack nitrate.
We have now added a section in the introduction that summarizes the reactive nitrogen and odd-nitrogen measurements in the Uintah Basin by Veres et al. [2015] and Wild et al. [2016].

Interestingly, there is also nitrite in the snow in the Uintah Basin, although at much lower levels than nitrate.
We now present our snow nitrite concentration measurements in Supplemental Material Figure 4A. Snow nitrite concentrations range from 0-14 ng g^{-1}, and are at least 3 to 5 orders of magnitude smaller than snow nitrate concentrations.

The arguments made about how reactive N sources changed with the various events seem weak, but could be made much stronger if the authors took advantage of the extensive measurements of gas phase N species made during this study.
We now use gas-phase N species measurements along with NOAA hysplit back trajectories to shed light on N-source changes during UBWOS2014, which further supports our hypothesis that the depleted $d^{15}N(NO_3^-)$ measurements at the snow surface on January 31 originated from deposition of nitrate formed outside the polluted Uintah basin. We've also included some additional discussion in the introduction and in section 3.1.1.

There are some gas-phase N species measurements with minimum daily-maximum mixing ratios immediately following the snow event on January 30/January 31. For example, Figure 7 in Veres et al. [2015] suggests that daily-maximum HO_2NO_2 mixing ratios during UBWOS2014 were relatively low after the snow event on January 30 and January 31, also corresponding to a sharp decrease in snow nitrite concentrations. In this manuscript, Figure 1B in Supplementary Material shows that daily-maximum gas and aerosol phase nitrate mixing ratios were also lowest immediately following the snow event.

Two-day NOAA HYSPLIT trajectories show that the air mass in the Uintah Basin on January 31 originated from the Pacific Ocean, which is distinctly different from the other air masses that reached the Uintah Basin during UBWOS2014 (see Supplemental Material, Figures 4B-15B). The large majority of air masses in the Uintah Basin during UBWOS2014 originated in the intermountain west and often centered over eastern Utah for several days.

Related to this, the authors refer several times to light or depleted N in background air. Is this a well-known aspect, or is there a hidden assumption at work here?
There have been a number of field campaigns designed to measure $\delta^{15}N$ of nitrate in ambient air. Morin et al. [2009] is an especially comprehensive study of background $\delta^{15}N$ that reports $\delta^{15}N$ measurements from many unpolluted regions in both the northern and southern hemisphere. The observation in Morin et al. [2009] show lighter $\delta^{15}N$ values in cleaner air masses, and heavier $\delta^{15}N$ values in more polluted air masses. This is mentioned in the manuscript near the end of the introduction.

It seems from the introduction, and references therein, that biological activity could also produce the same fractionation as the photolysis effect modeled here. Could the authors please explain how they have discounted this effect?
We have now added the following two sentences to the end of section 3.1.2:

"Emissions of microbial NO from subniveal soil could also lead to depleted $\delta^{15}N(NO_3^-)$ if this NO is oxidized to nitrate in the snowpack and deposited to the surface of snow grains before escaping to the atmosphere. However, the depleted $\delta^{15}N(NO_3^-)$ would also likely correspond with enhanced nitrate concentrations, which is not observed (Figures 3a-c). Additionally, calculations by Zatko et al. [2013] suggest that the lifetime of NO_x against oxidation to HNO_3 in snow interstitial air is long enough so that most NO emitted from soil microbial activity would likely be transported to the atmospheric boundary layer prior to oxidation."

Several places in the discussion the authors say that re-deposition of "light" nitrate accounts for the top layers seen in some profiles. This seems at odds with the conclusion that snow-derived light N is a small fraction of the reactive nitrogen source to the basin.

The re-deposition of isotopically-light nitrate is mentioned in the last paragraph of section 3.2.2. These lines describe a sensitivity study in which we have varied the quantum yield for nitrate photolysis (ϕ) in TRANSITS until there is a significant deviation between measured and modeled $\delta^{15}N(NO_3^-)$ profiles in snow. When $\phi = 0.2$, the model suggests that there is re-deposition of isotopically-light nitrate to the snow surface and enrichment in $\delta^{15}N(NO_3^-)$ with depth. When $\phi = 0.2$, the emissions of N_r from snow are still at least 7 times smaller compared to the N_r emissions from other sources within the Uintah Basin.

When the upper limit of ϕ is replaced with a more realistic ϕ in TRANSITS, there is considerably less re-deposition of isotopically-light nitrate to the snow surface in the Uintah Basin. Additionally, our measurements suggest that the $\delta^{15}N(NO_3^-)$ signature in the surface-snow layers is dominated by the deposition of nitrate from primary sources in the basin, and from sources beyond the basin during snow events.

Specific Comments

Line 61: "source of snow-sourced Nr" seems a bit awkward, how about just "source of Nr", you've already said it's from the snow.
We have removed "snow-sourced" from this sentence.

Line 99: O3 precursor emissions aren't necessarily higher in the summer. It is usually the stagnant summer high pressure events that contribute by limiting advection.
This sentence now reads:

"Maximum boundary layer O_3 concentrations are typically observed during the summer in major cities, where O_3 precursors are abundant and when conditions favor efficient O_3 production (high ultraviolet (UV) radiation) and air stagnation."

Lines 118-123 or so: The authors have not explained that these stable "build-up" events usually end when a storm front comes through, often dropping snow.
We have now added this sentence in the introduction:

"O_3 exceedance events end when stable boundary layers are disrupted by the passage of storm fronts, which often deposit snow".

Line 167: The pKa of HONO is about 2.9. Would the snow surface ever approach that and if it did would direct volatilization of HONO be a Nr loss mechanism? Does this equilibrium have an isotope effect?
Figure 3A presents estimates of snow pH based upon ion measurements made during UBWOS2014. The estimated pH of surface snow is typically between 2 and 4.

We have added a note about acidity in the introduction which reads:

"Under acidic conditions ($pk_a < 2.8$), aqueous–phase HONO can also be transferred to the gas phase (HONO (aq) ←→ HONO (g)) [*Anastasio and Chu*, 2009] and released into the boundary layer, where it can photolyze to produce gas-phase NO and OH [*Zhou et al*., 2001]."

We have also added the following sentence in section 4.2:

"The surface snow pH ranged from 2-4 during the campaign (see Figure 3A in Supplemental Material), which is low enough to enable direct volatilization of HONO from the snow."

We are unaware of any studies that reveal information about the isotopic effect associated with HONO volatilization. Frey et al. [2009] show that nitrate volatilization has an order of magnitude smaller N-isotope fractionation compared to photolysis, and it is likely that HONO volatilization has a similarly small isotope effect.

Lines 202-204: The authors mention all these processes that can influence 15N abundance but give no information about what direction or the magnitude.
Since $\delta^{15}N$ is a ratio of the abundance of $\delta^{15}N$ in a sample compared to reference material (N_2 in air), the $\delta^{15}N$ values associated with these processes do provide information about both the direction and magnitude of the enrichment/depletion of "heavy" nitrogen in a sample compared to the standard. For example, soil microbial activity tends to deplete (direction) samples of heavy nitrogen by 20 to 50 parts per thousand (magnitude), which is described as -50‰ to -20‰.

Line 449: How does a cascade impactor provide a measurement of HNO3, which I presume is gas phase nitric acid?
Thank you for catching this error. The cascade impactor only provides measurements of aerosol phase nitrate. This has been fixed in the manuscript.

Lines 721-723: Here is where the inconsistency really rears its head. How can "light snow- sources nitrate" have such an impact if it is a small fraction of N emitted to the basin?
Please see our response above to the comment about re-deposition of light nitrate to the snow surface layer being at odds with the conclusion that snow-derived light N is a small fraction of the reactive nitrogen source to the basin.

Line 739: The smoke stack does not extend above the boundary layer, the buoyancy of the warmer plume causes the emissions to settle in a layer just above the cold boundary layer.

This sentence now reads:

"The power plant is excluded because its emissions occur above the boundary layer due to the plume's positive buoyancy."

References:

Anastasio, C. and Chu, L.: Photochemistry of nitrous acid (HONO) and nitrous acidium ion (H_2ONO^+) in aqueous solution and ice. *Environ. Sci. Tech*., 43, 1108-1114, 2009.

Frey, M.M., Savarino, J., Morin, S., Erbland, J., Martins, J.M.F.: Photolysis imprint in the nitrate stable isotope signal in snow and atmosphere of East Antarctica and implications for reactive nitrogen cycling. *Atmos. Chem. Phys*., 9, 8681-8696, 2009.

Morin, S., Savarino, J., Frey, M.M., Domine, F., Jacobi, H.-W., Kaleschke, L., Martins, J.M.F.: Comprehensive isotopic composition of atmospheric nitrate in the Atlantic Ocean boundary layer from 65°S to 79°N. J. *Geophys. Res*., 114, D05303, doi:10.1029/208JD010696, 2009.

Veres, P.R., Roberts, J.M., Wild, R.J., Edwards, P.M., Brown, S.S., Bates, T.S., Quinn, P.K., Johnson, J.E., Zamora, R.J., de Gouw, J.: Peroxynitric acid (HO2NO2) measurements during the UBWOS 2013 and 2014 studies using iodide ion chemical ionization mass spectrometry. *Atmos. Chem. Phys*., 15, 8101-8114, doi:10.5194/acp-15-8101-2015, 2015.

Wild, R.J., Edwards, P.M., Bates, T.S., Cohen, R.C., deGouw, J.A., Dube, W.P., Gilman, J.B., Holloway, J., Kercher, J., Koss, A.R., Lee, L., Lerner, B.M., McLaren, R., Quinn, P.K., Roberts, J.M., Stutz, J., Thornton, J.A., Veres, P.R., Warneke, C., Williams, E., Young, C.J., Yuan, B., Zarzana, K.J., Brown, S.S.: Reactive nitrogen partitioning and its relationship to winter ozone events in Utah. *Atmos. Chem. Phys*., 16, 573-583, doi:10.5194/acp-16-573-2016, 2016.

Zatko, M.C., Grenfell, T.C., Alexander, B., Doherty, S.J., Thomas, J.L., Yang, X., The influence of snow grain size and impurities on the vertical profiles of actinic flux and associated NOx emissions on the Antarctic and Greenland ice sheets. *Atmos. Chem. Phys*., 13, 3547-3567, doi:10.5194/acp-13-3547-2013, 2013.

Zhou, X., Beine, H.J., Honrath, R.E., Fuentes, J.D., Simpson, W., Shepson, P.B., Bottenheim, J.W.: Snowpack photochemical production of HONO: a major source of OH in the Arctic boundary layer in springtime. *Geophys. Res. Lett*., 28(21), 4087-4090, 2001.

Author Response to Reviewer 2:

We thank Reviewer 2 for their helpful comments and suggestions**.**

The manuscript of Zatko et al uses measured snow nitrate concentrations along with nitrogen isotopes to infer the flux of reactive nitrogen from irradiated snowpack and compare the magnitude of this flux to other nitrogen sources within the Uintah Basin. It was determined that the reactive nitrogen flux from snow was minimal when compared to the much larger anthropogenic NOx (primary) sources within the basin. Studies of this nature are important to constrain reactive nitrogen sources, as well as to better understand ground-level ozone chemistry, which has been shown to be impacted by the presence of snowpack in winter in the Uintah Basin. The data presented are unique and high quality and will be of potential broad interest to ACP readership. The measurement and modeling methods used are appropriate and justified. The results, for the most part, support the interpretations and conclusions made (with a few questions I present below that could use clarification). However I think some improvements in organization and presentation would significantly strengthen the manuscript, as outlined below.

1) In the current form, the manuscript is a bit unwieldy and verbose. I think much of the language can be tightened up and the overall length of the manuscript shortened without losing meaning.
We have shortened this manuscript by roughly 3 pages overall by reducing repetition. The results and conclusions sections are most drastically reduced in length, but there have been reductions in the introduction and methods sections as well.

2) During the first read, my first impression was that it was dominated by experimental and model descriptions. I kept asking myself "when do we get to the good stuff?" The major focus of the results is predicated on the nitrate concentrations and isotope results, so I would suggest cutting back on the details of the other measurements (perhaps moving to supplemental?) and summarizing more succinctly those results within the discussion.
We have removed some material from the methods sections and have also removed some repetition about nitrate concentrations and isotopes from the results. A novel approach is used in this study to assess photochemistry in mid-latitude regions. Since this approach relies heavily on both optical and chemical models and measurements, and is the first of its kind, we feel that it is appropriate to include thorough descriptions of the approach.

We think it would be most preferable to keep the methods section in tact rather than placing parts of it in a supplemental section. We leave it to the editor to decide if we should shorten the methods section further by moving some information to the supplement. The results section highlights snow-sourced N_r fluxes, which are all dependent on the field measurements, laboratory techniques, and modeling tools used in this study. Since the flux of N_r is dependent on both optical and chemical measurements, we think it would be misleading to focus on one just one of these aspects in the methods section. Lastly, both of the models used in this analysis rely heavily on optical and

chemical measurements and we feel that it is beneficial for readers to understand the link between measurements and the models.

3) Throughout the manuscript there are references to gas phase N chemistry, changing sources, etc but no mention of e.g. gas phase NOx measurements, magnitudes, etc. I presume there are coupled gas phase measurements that were made by someone during the field campaign? If so, bringing them into the discussion (with back trajectories?) could help strengthen arguments about deposition of nitrate from less polluted regions surrounding the basin, etc.
We have now added a section in the introduction that summarizes the reactive nitrogen and odd-nitrogen measurements in the Uintah Basin made by Veres et al. [2015] and Wild et al. [2016]. We have also added some discussion in section 3.1.1 that uses gas-phase N-species measurements and NOAA HYSPLIT back trajectories to shed light on N-source changes during UBWOS2014.

The gas-phase measurements made during the UBWOS campaigns in the Uintah Basin are subject to diurnal patterns of boundary layer mixing [Lee et al., 2014], which add a layer of complexity to interpreting reactive N measurements. Figure 7 in Veres et al. [2015] does suggests that daily-maximum HO_2NO_2 mixing ratios during UBWOS2014 were relatively low after the snow event on January 30 and January 31, also corresponding to a sharp decrease in snow nitrite concentrations. In this manuscript, Figure 1B in Supplementary Material shows that daily-maximum gas and aerosol phase nitrate mixing ratios were also lowest immediately following the snow event.

Two-day NOAA HYSPLIT trajectories show that the air mass in the Uintah Basin on January 31 originated from the Pacific Ocean, which is distinctly different from the other air masses that reached the Uintah Basin during UBWOS2014 (see Supplemental Material, Figures 4B-15B). The large majority of air masses in the Uintah Basin during UBWOS2014 originated in the intermountain west and often centered over eastern Utah for several days.

4) Do you have measurements of nitrite in the snow? It's been shown that the nitrite photolysis channels can also be a significant source of nitrogen oxides from snow (see e.g. Jacobi et al., EST, 2014 based from Barrow, AK). It doesn't appear this is included in your flux calculations/model, only the nitrate channel (reaction E1). A quick sensitivity study could help you rule in/out the importance of reactions E3-E5.
We do have measurements of nitrite in snow and have presented this data in Figure 4A in Supplemental Material A. Snow nitrite concentrations range from 0-14 ng g^{-1}, and are at least 3 to 5 orders of magnitude smaller than snow nitrate concentrations (Figure 3). Although nitrite photolyzes across a wider wavelength range compared to nitrate, since snow nitrite concentrations are significantly lower compared to snow nitrate concentrations, it is likely that nitrate photolysis is the dominant source of snow-sourced nitrogen oxides in the Uintah Basin.

Additionally, since nitrate photolysis is responsible for the formation of nitrite in snow, nitrite photolysis can be somewhat viewed as an intermediary reaction associated with nitrate photolysis, especially since both the major and minor channels of nitrate photolysis produce nitrogen oxides.

5) Related to the idea of shortening the paper – is Figure 3 necessary? Essentially the same data are presented in Figure 8 as well. Also, figures 2, 4 and 5 could potentially be combined into a multi-panel figure.
Figure 8 is now Figure 3 so that we avoid showing the snow nitrate concentrations and isotopes twice. We have also combined Figures 4 and 5.

6) From the methods, it appears you quantified BC and LAI via absorption properties, rather than actual chemical measurements (e.g. EC/OC, DOC, etc). As such, I would question the wording of lines 598-599 where you state "concentrations of LAI in the snow photic zone are at least five orders of magnitude higher in Utah compared to Antarctica and Greenland". While I do not doubt there are more light absorbing species in Utah v Antarctica, unless it is based on chemical measurements it is misleading to relate this directly to concentrations. Same argument goes for lines 616-617. The absorption cross sections might just be very different amongst sites/times, while concentrations might not be orders of magnitude different. If you do have measurements of DOC, etc it would be very useful to include reference to these.
During the campaign we filtered melted snow through a filter designed to trap insoluble light-absorbing particles, such as black carbon, brown carbon, organics, and dust. We used an optical technique to estimate the concentration of black carbon in each snow sample (see Figures 2a,c,e), which is an alternative approach to combustion-based measurements. Although we are able to estimate black carbon concentrations using this technique, you are correct that this method does not provide direct concentration estimates of other light absorbers, such as organic carbon. Instead, using this technique we are able to estimate the fraction of UV light absorption by nonBC species compared to BC species.

While we do have BC concentration estimates, since we do not have direct concentration measurements of nonBC species, we agree that the wording of these lines should be changed. We have replaced “concentrations of LAI” and “LAI concentrations” with “UV absorption by LAI” in these lines.

7) Line 616: reword as "concentrations in the surface layer". . .
This sentence has been reworded and “concentrations” have been replaced with “UV absorption by LAI”.

8) At line 623 I would redefine F(Nr(z)) since you haven’t mentioned it since beginning of manuscript.
We have redefined $F_{Nr}(z)$ in this sentence.

9) Line 712: correct the wording, choose either "differ by" or "vary by"
This sentence is no longer in our manuscript.

References:

Veres, P.R., Roberts, J.M., Wild, R.J., Edwards, P.M., Brown, S.S., Bates, T.S., Quinn, P.K., Johnson, J.E., Zamora, R.J., de Gouw, J.: Peroxynitric acid (HO2NO2) measurements during the UBWOS 2013 and 2014 studies using iodide ion chemical ionization mass spectrometry. *Atmos. Chem. Phys*., 15, 8101-8114, doi:10.5194/acp-15-8101-2015, 2015.

Wild, R.J., Edwards, P.M., Bates, T.S., Cohen, R.C., deGouw, J.A., Dube, W.P., Gilman, J.B., Holloway, J., Kercher, J., Koss, A.R., Lee, L., Lerner, B.M., McLaren, R., Quinn, P.K., Roberts, J.M., Stutz, J., Thornton, J.A., Veres, P.R., Warneke, C., Williams, E., Young, C.J., Yuan, B., Zarzana, K.J., Brown, S.S.: Reactive nitrogen partitioning and its relationship to winter ozone events in Utah. *Atmos. Chem. Phys*., 16, 573-583, doi:10.5194/acp-16-573-2016, 2016.

The magnitude of the snow-sourced reactive nitrogen flux to the boundary layer in the Uintah Basin, Utah, USA

Maria Zatko[1], Joseph Erbland[2,3], Joel Savarino[2,3], Lei Geng[1,a], Lauren Easley[4], Andrew Schauer[5], Timothy Bates[7], Patricia K. Quinn[6], Bonnie Light[8], David Morison[8,b], Hans D. Osthoff[9], Seth Lyman[10], William Neff[11], Bin Yuan[11,12], Becky Alexander[1]

[1]Department of Atmospheric Sciences, University of Washington, Seattle, 98195, USA
[2]Université Grenoble Alpes, LGGE, 38000 Grenoble, France
[3]CNRS, LGGE, 38000 Grenoble, France
[4]Department of Chemistry, University of Washington, Seattle, Washington, 98195, USA
[5]Earth and Space Sciences, University of Washington, Seattle, Washington, 98195, USA
[6]Pacific Marine Environmental Laboratory, National Oceanic and Atmospheric Administration, Seattle, Washington, 98115, USA
[7]Joint Institute for the Study of the Atmosphere and Oceans, University of Washington, Seattle, Washington, 98195, USA
[8]Polar Science Center, Applied Physics Laboratory, University of Washington, Seattle, Washington, 98195, USA
[9]Department of Chemistry, University of Calgary, 2500 University Drive NW, Calgary, AB T2N 1N4, Canada
[10]Bingham Entrepreneurship and Energy Research Center, Utah State University, 320 Aggie Boulevard, Vernal, Utah, 84078, USA

[11]Cooperative Institute for Research in the Environmental Sciences, University of Colorado, Boulder, Colorado, 80309, USA

[12]Chemical Sciences Division, Earth System Research Laboratory, National Oceanic and Atmospheric Administration, Boulder, Colorado, 80305, USA

[a]Now at Université Grenoble Alpes, LGGE, 38000 Grenoble, France, CNRS, LGGE, 38000 Grenoble, France

[b]Now at Department of Physics and Astronomy, University of Utah, Salt Lake City, Utah, 84112, USA

Correspondence to Becky Alexander (beckya@uw.edu)

Abstract

Reactive nitrogen (N_r=NO, NO_2, HONO) and volatile organic carbon emissions from oil and gas extraction activities play a major role in wintertime ground-level ozone exceedance events of up to 140 ppb in the Uintah Basin in eastern Utah. Such events occur only when the ground is snow covered, due to the impacts of snow on the stability and depth of the boundary layer and ultraviolet actinic flux at the surface. Recycling of reactive nitrogen from the photolysis of snow nitrate has been observed in polar and mid-latitude snow, but snow-sourced reactive nitrogen fluxes in mid-latitude regions have not yet been quantified in the field. Here we present vertical profiles of snow nitrate concentration and nitrogen isotopes ($\delta^{15}N$) collected during the Uintah Basin Winter Ozone Study 2014 (UBWOS 2014), along with observations of insoluble light-absorbing impurities, radiation equivalent mean ice grain radii, and snow density that determine snow optical properties. We use the snow optical properties and nitrate concentrations to calculate ultraviolet actinic flux in snow and the production of N_r from the photolysis of snow nitrate. The observed $\delta^{15}N(NO_3^-)$ is used to constrain modeled fractional loss of snow nitrate in a snow chemistry column model, and thus the source of N_r to the overlying boundary layer. Snow-surface $\delta^{15}N(NO_3^-)$ measurements range from -5‰ to 10‰ and suggest that the local nitrate burden in the Uintah Basin is dominated by primary emissions from anthropogenic sources, except during fresh snowfall events, where remote NO_x sources from beyond the basin are dominant. Modeled daily-averaged snow-sourced N_r fluxes range from 5.6-71x10^7 molec cm^{-2} s^{-1} over the course of the field campaign, with a maximum noon-time value of 3.1x10^9 molec cm^{-2} s^{-1}. The top-down emission estimate of primary, anthropogenic NO_x in the Uintah and Duchesne counties is

Maria Zatko 7/11/16 9:00 PM
Deleted: snow-sourced

70 at least 300 times higher than the estimated snow NO_x emissions presented in this study.
71 Our results suggest that snow-sourced reactive nitrogen fluxes are minor contributors to
72 the N_r boundary layer budget in the highly-polluted Uintah Basin boundary layer during
73 winter 2014.
74
75
76
77
78
79
80
81
82
83
84
85
86
87
88
89
90

1. Introduction

Ozone (O_3) has adverse respiratory effects, is an effective greenhouse gas [*UNEP*, 2011], and, through formation of the hydroxyl radical, influences the oxidizing capacity of the atmosphere [*Thompson,* 1992]. O_3 precursors include volatile organic compounds (VOCs) emitted from vegetation, biomass burning, and fossil fuel combustion [*Guenther et al*., 1995, *Warneke et al*., 2014] and nitrogen oxides (NO_x=NO+NO_2) emitted from fossil fuel combustion, biomass burning, soil microbial activity, lightning, and photochemical reactions in snow [*Delmas et al*., 1997, *Grannas et al*., 2007, *Logan et al*., 1983]. Maximum boundary layer O_3 concentrations are typically observed during the summer in major cities, where O_3 precursors are abundant and when conditions favor efficient O_3 production (high ultraviolet (UV) radiation) and air stagnation. High O_3 concentrations in the boundary layer exceeding 100 ppbv were measured in winter 2005 in the Upper Green River Basin in rural Wyoming [*Schnell et al*., 2009], well above the current Environmental Protection Agency (EPA) National Ambient Air Quality Standard (NAAQS) 8-hour average limit of 70 ppbv. High wintertime O_3 episodes have also been observed in the Uintah Basin in rural Utah [*Martin et al*., 2011], and in both basins, these O_3 episodes only occur when the ground is snow-covered [*Oltmans et al*., 2014]. The Upper Green River Basin and the Uintah Basin are regions of major oil and gas development, and the production of oil and natural gas in the Upper Green River Basin and the Uintah Basin is expected to increase through at least 2020 [*US EIA*, 2014].

These wintertime high O_3 episodes motivated a series of field campaigns, including the Upper Green Winter O_3 Study (UGWOS 2011, UGWOS 2012) and the Uintah Basin

Winter O_3 Study (UBWOS 2012, UBWOS 2013, UBWOS 2014). Results from these field campaigns [*Gilman et al*., 2013, *Helmig et al*., 2014, *Oltmans et al*., 2014, *Warneke et al*., 2014, *Schnell et al*., 2009] and subsequent modeling studies [*Ahmadov et al*., 2015, *Carter and Seinfeld*, 2012, *Edwards et al*., 2013, 2014, *Field et al*., 2015, *Rappengluck et al*., 2014] reveal that emissions of NO_x and VOCs from oil and gas extraction, combined with stagnant meteorological conditions, enhanced boundary layer UV radiation due to the high UV albedo of snow [*Warren et al*., 2006], and reduced O_3 loss through surface deposition due to snow cover [*Ahmadov et al*., 2015], trigger high boundary layer O_3 episodes in these basins. O_3 exceedance events occur only when the ground is snow covered because snow aids in the formation and maintenance of a stable air mass and reflects UV radiation upwards into the boundary layer. O_3 exceedance events end when stable boundary layers are disrupted by the passage of storm fronts, which often deposit snow. Modeling studies were used to determine whether O_3 formation in these regions is NO_x-sensitive or VOC-sensitive, which is necessary information for the enactment of effective regulations aimed to reduce boundary layer O_3 abundance. Modeling results from Edwards et al. [2014] suggest that the Uintah Basin is in an O_3 formation regime on the boundary between VOC-sensitive and NO_x-sensitive and modeling results from Ahmadov et al. [2015] suggest that the Uintah Basin regime is VOC-sensitive. Modeling results presented in Edwards et al. [2014] suggest that the dominant radical sources in the Uintah Basin are carbonyl compounds (85%), with smaller inputs from HONO, O_3, and nitryl chloride ($ClNO_2$) photolysis.

Atmospheric measurements in the Uintah Basin during UBWOS2012, UBWOS2013, and UBWOS2014 reveal that the total reactive nitrogen abundances (NO_y=NO+NO_2+HNO_3+PAN+N_2O_5+NO_3+$ClNO_2$+organic nitrates) are highest (12-24 ppbv) in 2013 due to persistent shallow inversion layers trigged by stagnant air masses and snow cover, lowest in 2012 (4-9 ppbv) when no snow covered the ground, and in-between (8-18 ppbv) in winter 2014, with the highest NO_y values generally in mid-day [*Wild et al*., 2016]. In 2013, HNO_3 accounted for nearly half of total NO_y while in 2012 N_2O_5 and $ClNO_2$ were larger components of total NO_y compared to HNO_3 [*Wild et al*., 2016]. Interestingly, atmospheric NO_x mixing ratios are similar in all three years, with diurnal averages ranging from 2 ppbv during the night to 10 ppbv during the day [*Wild et al*., 2016]. The NO_x/NO_y ratio, indicative of the rate of oxidation of reactive nitrogen, was highest in 2013 and lowest in 2012, with intermediate values in 2014 [*Wild et al*., 2016]. HO_2NO_2 measurements range from 0 to 2.4 ppbv in 2013 and ~0 to 0.4 ppbv in 2014 [*Veres et al*., 2015] and are generally positively correlated with snow nitrite concentrations, suggesting that HO_2NO_2 deposition may be a source of snow nitrite [*Veres et al*., 2015].

In addition to aiding in the formation and maintenance of a stable air mass with enhanced UV radiation, snow may also recycle reactive nitrogen oxides (N_r = NO_x, HONO) between the snow surface and the overlying atmosphere, effectively increasing the atmospheric lifetime of N_r. The major sink of N_r in the atmosphere is the formation and deposition of nitrate (particulate NO_3^- plus HNO_3(g)). When nitrate is deposited to snow, its photolysis serves to recycle N_r to the overlying boundary layer [*Grannas et al.,* 2007,

159 *Honrath et al*., 2000]. This snow-sourced N_r can then be re-oxidized to nitrate and re-
160 deposited to the snow surface. The recycling of nitrogen between the snow surface and
161 boundary layer can occur many times, resulting in the continuous recycling of N_r during
162 sunlit conditions.
163
164 The photolysis of nitrate occurs in the liquid-like region (LLR) in or on ice grains
165 [*Domine et al*., 2013] in the top snow layer where UV radiation is present, which is
166 known as the snow photic zone. Snow nitrate photolyzes at wavelengths (λ)=290-345 nm
167 to produce aqueous-phase nitrogen dioxide (NO_2) or nitrite (NO_2^-) according to E1 and
168 E2 [*Grannas et al*., 2007, *Mack and Bolton*, 1999, *Meusinger et al*., 2014].
169
170 $NO_3^-(aq) + h\nu(+H^+) \rightarrow NO_2(aq) + OH(aq)$, E1
171 $NO_3^-(aq) + h\nu \rightarrow NO_2^-(aq) + O(^3P)(aq)$, E2
172
173 The measured quantum yields (ϕ) for E1 range from 0.003-0.6 molec photon^{-1} at 253 K
174 [*Chu and Anastasio*, 2003, *Meusinger et al*., 2014, *Zhu et al*., 2010], and is likely
175 influenced by the location of nitrate within ice grains. The NO_2 produced in E1 quickly
176 evaporates due to its low solubility and can be transported to the overlying atmosphere.
177 The nitrite produced in E2 is rapidly photolyzed at longer wavelengths (λ=290-390 nm)
178 (E3).
179
180 $NO_2^-(aq) + h\nu(+H^+, aq) \rightarrow NO(aq) + OH(aq)$, E3
181

Nitrite can also react with OH or H^+ in the LLR to produce aqueous-phase NO_2 and HONO [*Grannas et al.*, 2007]:

$NO_2^-(aq) + OH(aq) \rightarrow NO_2(aq) + OH^-(aq)$, E4

$NO_2^-(aq) + H^+(aq) \rightarrow HONO(aq)$, E5

HONO can rapidly photolyze in the LLR to produce aqueous-phase NO and OH [*Anastasio and Chu*, 2009]; due to its short lifetime the aqueous-phase OH remains in the LLR, but the aqueous-phase NO can be transferred to the gas phase and ultimately be released into the boundary layer. Under acidic conditions ($pk_a < 2.8$), aqueous-phase HONO can also be transferred to the gas phase (HONO (aq) ←→ HONO (g)) [*Anastasio and Chu*, 2009] and released into the boundary layer, where it can photolyze to produce gas-phase NO and OH [*Zhou et al.*, 2001].

Nitrate nitrogen isotopes ($\delta^{15}N(NO_3^-)$) in the air and snow can provide useful information about snow photochemistry, specifically, the degree of photolysis-driven recycling and loss of nitrate from the snow. Nitrogen isotope ratios are expressed as $\delta^{15}N$, where $\delta = R_{sample}/R_{reference} - 1$, $R = {}^{15}N/{}^{14}N$, and N_2-air is the reference material. Nitrate photolysis in snow is a mass-dependent process and is associated with a large fractionation constant (ε) of -47.9‰ at wavelengths shorter than 320 nm [*Berhanu et al.*, 2014]. Nitrate photolysis provides the boundary layer with a source of N_r that is highly depleted in ^{15}N, leaving highly enriched $\delta^{15}N(NO_3^-)$ deeper in the snow. Snow-sourced nitrate that is redeposited to the snow surface is lighter than the remaining nitrate in the snow, leading to $\delta^{15}N(NO_3^-$

Maria Zatko 7/24/16 10:08 AM
Deleted: A

Maria Zatko 7/24/16 10:10 AM
Formatted: Subscript

Maria Zatko 7/24/16 10:09 AM
Formatted: Font:Italic

Maria Zatko 7/12/16 7:21 AM
Deleted:

Maria Zatko 7/12/16 7:21 AM
Deleted: ... [1]

Maria Zatko 8/10/16 7:38 AM
Deleted: a

) values that become more enriched with increasing depth within the snow photic zone. $\delta^{15}N(NO_3^-)$ values in the atmosphere are also influenced by the relative importance of different NO_x sources [see *Felix and Elliott,* 2014 for a summary]. For example, the atmospheric $\delta^{15}N$ signature from anthropogenic NO_x sources, such as combustion of fossil fuels, range from -19.0‰ to 25.0‰ [*Felix et al.,* 2012, *Walters et al*., 2015]. The $\delta^{15}N$ signature from soil microbial activity is generally lower than that of anthropogenic activity and ranges from -50‰ to -20‰ [*Felix and Elliott*, 2014]. Observations of atmospheric $\delta^{15}N(NO_3^-)$ in non-polluted, mid-latitude regions range from -6 to -2‰, while $\delta^{15}N(NO_3^-)$ values measured in polluted regions range from 0 to 6‰ [*Morin et al*., 2009]. In addition, atmospheric $\delta^{15}N(NO_3^-)$ is influenced by NO_x cycling [*Freyer et al*., 1993; *Walters et al*., 2016], NO_2 oxidation [*Walters and Michalski*, 2015], and the partitioning of nitrate between its gas and particulate phases [*Heaton et al*., 1997].

In this study, we investigate the importance of snow photochemistry as a source of reactive nitrogen oxides to the boundary layer in the Uintah Basin using chemical, isotopic, and optical measurements from the snow collected during the UBWOS 2014 campaign. In Section 2 we describe the field, laboratory, and modeling techniques used in this study. In Section 3 we present the chemical and optical measurements made during UBWOS 2014 and model-calculated fluxes of snow-sourced N_r. In Section 4 we estimate the contribution of snow-sourced N_r to the N_r burden in the Uintah Basin boundary layer.

Maria Zatko 7/12/16 7:22 AM

Deleted: We use these observations of snow optical properties along with observations of surface downwelling irradiance as inputs to a snow radiative transfer model to calculate photolysis frequencies in the snow. The source of snow N_r is then calculated simply by multiplying the calculated photolysis frequencies by the observed snow nitrate concentrations. The calculated photolysis frequencies in snow are also used in a snow photochemistry column model which is constrained by our observations of snow $\delta^{15}N(NO_3^-)$.

2. Methods

2.1. Field and Laboratory Observations

2.1.1. UBWOS 2014 Field Site Description and Meteorological Conditions

UBWOS 2014 occurred from January 17, 2014 to February 13, 2014 at the Horsepool field-intensive site (40.1°N, 109.5°W) in the Uintah Basin, roughly 35 miles south of Vernal, Utah. There are over 10,000 oil and natural gas wells in the basin connected by a series of dirt roads. The meteorological conditions were relatively constant for most of the campaign; wind speeds ranged from 1 to 3 m s^{-1} and often originated from the southwest. Sky conditions were clear, temperatures ranged from 258 to 275 K, and boundary layer heights generally ranged from 25 to 150 m. There were a few cloudy days (January 29-February 4, February 10) during the campaign and the last several days experienced temperatures above freezing. Daily maximum boundary layer O_3 mixing ratios ranged from 45 ppb to 90 ppb, and the campaign-averaged daily-maximum boundary layer O_3 mixing ratio was 61 ppb.

Snow covered the ground throughout the duration of the campaign, and ranged in depth from 10 to 30 cm, depending on how snow was redistributed by wind after deposition. The snow was deep enough to cover some of the lowest-lying vegetation, but branches from bushes were still visible. Three snow events occurred before the campaign, one event on December 4, which deposited most of the snow (19 cm), and two smaller events on December 8 and December 19, which deposited roughly 3 cm and 1 cm of snow,

267 respectively. There was a distinct crust layer roughly 4 cm below the snow surface,
268 providing evidence of surface melting between the later two snowfall events. The
269 temperature difference between the soil and the air was at least 15 K for several weeks,
270 allowing vapor to redistribute through the snow, leading to the formation of large hoar
271 crystals (radiation equivalent mean ice grain radii [*Hansen and Travis*, 1974] (r_e) > 1200
272 μm) at all depths in the snow. There was one major snow event during the campaign on
273 January 30 through January 31 that deposited roughly 5 cm of fresh snow (r_e ~ 100 μm).
274 There were two smaller snow events on February 4 and February 10. On February 4 there
275 was no measureable snow accumulation and during the early-morning hours of February
276 10 there was 2 cm of fresh snow that subsequently melted several hours after sunrise.
277 Supplementary Figure 3B summarizes daily snow accumulation before and during the
278 campaign.
279
280 **2.1.2 Snowpit Measurements and Snow Sample Preparation**
281 Twelve snowpits were dug approximately every 2 to 3 days during the campaign.
282 Snowpits were dug from the snow surface to about 1 cm above the subniveal ground and
283 ranged in depth from 9 to 24 cm. The snowpits were dug in a variety of directions
284 roughly 150 meters from the main Horsepool site, except for snowpit 5 (January 24),
285 which was dug roughly 800 meters away from Horsepool. The snowpits were dug
286 wearing clean, nitrate-free gloves using a stainless steel spatula. For each snowpit,
287 vertical profiles (1-cm depth resolution) of snow density (ρ_{snow}), temperature, and
288 radiation equivalent ice grain radii (r_e) were measured using a Taylor-LaChapelle snow
289 density kit, a dial stem thermometer, and a laminated snow grid card with 1 mm grid

Maria Zatko 7/12/16 7:22 AM
Deleted: and measured

spacing, respectively. Snow grains from each distinct snow layer were placed on the snow grid card and a photograph was taken. The photographs were projected onto a larger screen and the shortest dimension of each snow crystal was estimated. The shortest dimension of a snow grain is the most optically important dimension [*Grenfell and Warren*, 1999], and in this study, it is used to represent r_e. For hoar crystals, the smallest dimension is the width of the crystal wall and for freshly-fallen crystals, the smallest dimension is the radius of the rounded crystal. For each snowpit, approximately 1 kg of snow was collected at 1-cm depth intervals and placed into 'whirl-pak' plastic bags. The bags were kept covered while in the field and then immediately placed into a freezer once back at the Utah State University (USU) Uintah Basin Campus in Vernal, Utah. Supplementary section A shows detailed information on each snowpit.

2.1.3. Optical Measurements

The snow from each plastic bag was spooned into a clean glass beaker and melted in a microwave oven at USU. The meltwater was transferred to a stainless steel funnel and passed through a 0.4 μm Nuclepore filter, using an electric diaphragm vacuum pump to create a partial vacuum in a volumetric flask. The Nuclepore filter collects insoluble light absorbing impurities (LAI) in snow, including black carbon (BC) and non-black carbon (non-BC) species, the latter of which encompass brown carbon, dust, and organics. The volume of filtrate was measured, which ranged from 40 to 750 ml depending on impurity content. After the Nuclepore filters dried overnight, the filters were frozen until further analysis at the University of Washington (UW).

The absorption spectrum of each Nuclepore filter was measured using an ISSW spectrophotometer [*Grenfell et al*., 2011] in the Arctic Snow Laboratory at UW. The Nuclepore filter is placed between two integrating spheres lined with Spectralon material to create a fully diffuse medium. An Ocean Optics USB-650 spectrophotometer is used to measure the absorption spectrum in units of optical depth, $\tau(\lambda)$ (dimensionless, e.g. cm^2 cm^{-2}), from λ=350-1000 nm in 10 nm intervals. A set of standard filters containing known loadings of black carbon (Fullerene) is used to calibrate the ISSW spectrophotometer. The spectral absorption measured by the spectrophotometer for each filter is characterized by an Ångstrom exponent ($\mathring{A}$), which represents the total absorption by both BC and non-BC LAI on the filter between two visible wavelengths. $\mathring{A}$ is calculated in E7:

$$\mathring{A}(\lambda_1 \; to \; \lambda_2) = \frac{\ln\left(\frac{\tau(\lambda_1)}{\tau(\lambda_2)}\right)}{\ln\left(\frac{\lambda_2}{\lambda_1}\right)} \;, \qquad \text{E7}$$

where λ_1=450 nm and λ_2=600 nm. The λ=450-600 nm range is chosen because the ISSW spectrophotometer signal is most stable over this wavelength range. The total absorption Ångstrom exponent on each filter along with assumed Ångstrom exponents for BC ($\mathring{A}$=1) and non-BC ($\mathring{A}$=5) are used to estimate snow BC concentrations and the fraction of ultraviolet (λ=300-350 nm) absorption by non-BC material (see *Doherty et al*., 2010, *Grenfell et al*., 2011, *Zatko et al*., 2013, and *Zatko and Warren*, 2015). Triplicate measurements were performed for all samples.

Surface upwelling and downwelling irradiance was measured using a commercial spectral radiometer equipped with a photodiode array (Metcon GMBH,

http://www.metcon-us.com). Upwelling and downwelling UV-A and UV-B were measured with Kipp and Zonen Model UV-S-AB-T radiometers. Radiometers were placed at 2 m above ground (one up-facing and one down-facing) and were cleaned and checked weekly to ensure that the radiometers remained directly perpendicular to the ground. Detailed irradiance data is provided in the Supplemental Material.

2.1.4. Chemical Concentration and Nitrate Isotopic Measurements

In a laboratory on the USU campus in Vernal, UT, a 50 µl aliquot of snow meltwater that was passed through the Nuclepore filter was used to measure ion (Cl^-, Br^-, NO_3^-, SO_4^{2-}, Na^+, NH_4^+, K^+, Mg^{+2}, Ca^{+2}, oxalate) concentrations using a Metrohm 761 Compact Ion Chromatograph Analyzer [*Quinn et al*., 1998]. The nitrate in the remaining filtrate was preconcentrated for isotopic analysis. Nitrate was preconcentrated by passing the meltwater through an anion exchange resin (BioRad AG 1-X8) using an electric diaphragm pump. The sample anions in the resin were eluted with 5x2 ml 1 M sodium chloride (NaCl/Milli-Q water) solution into a 30 ml pre-cleaned sample bottle. This method has been shown to ensure full recovery of nitrate [*Silva et al*., 2000, *Frey et al*., 2009] The solution was kept frozen in the dark until analysis in the University of Washington IsoLab (http://isolab.ess.washington.edu/isolab/).

The denitrifier method [*Casciotti et al*., 2002, *Kaiser et al*., 2007, *Sigman et al*., 2001] was used to determine the nitrogen isotopic signature ($\delta^{15}N$) in each snow sample. Denitrifying bacteria, *Pseudomonas aureofaciens,* convert nitrate to nitrous oxide (N_2O) gas in anaerobic conditions [*Casciotti et al*., 2002, *Sigman et al*., 2001] and N_2O is

transported via helium gas through a heated gold tube (800°C), where it thermally decomposes into O_2 and N_2. After separation by gas chromatography, the O_2 and N_2 are run through a Thermo Finnigan^{TM} DeltaPlus Advantage isotope ratio mass spectrometer (IRMS), equipped with a Precon and GasBench II^{TM}. The $\delta^{15}N$ values were calculated with respect to N_2 (air) via two international reference materials USGS32 ($\delta^{15}N$ =180‰) and USGS34 ($\delta^{15}N$ =-1.8‰), with IAEA ($\delta^{15}N$ =4.7‰) as a quality control standard. For many samples, the $NaCl/NO_3^-$ solution was diluted with Milli-Q water to obtain the optimal nitrate concentration (200 nmol in 2 ml) for each sample run on the IRMS. Triplicate measurements were performed for all samples. The analytical uncertainty of $\delta^{15}N(NO_3^-)$ (1σ) was 0.75‰ based on repeated measurements of the quality control standard.

Aerosol nitrate was collected throughout the campaign in 12-hour intervals. Aerosol nitrate was sampled from an inlet 13 meters above ground and drawn through a heated (283K) pipe, where it was then collected on a two-stage, multi-jet cascade impactor. The impactor tedlar films separates aerosols with diameters less than 2.5 μm from those with diameters between 2.5 to 12.5μm. The aerosols were extracted from the filters and analyzed using ion chromatography, following methods described in Quinn et al. [2000]. Gas-phase nitric acid was measured using an Acetate HR-ToF-CIMS instrument throughout the campaign with 1-minute time resolution, as described in Yuan et al. [2016].

2.2. Calculations

383

384 **2.2.1. Snow Radiative Transfer Model**

385 A 4-stream, plane-parallel radiative transfer model using the discrete ordinates method
386 with a δ-M transformation originally described in Grenfell et al. [1991] was used to
387 calculate vertical profiles of UV actinic flux in each snowpit. This model properly treats
388 layers with differing refractive indices and the 4-stream model produces albedo and
389 absorptivity results that agree to within 1% of higher-order models representative of snow
390 [*Wiscombe*, 1977], including DISORT [*Stamnes et al*., 1988]. Vertical profiles of the
391 ρ_{snow}, r_e, and LAI absorption are used to calculate vertical profiles of inherent optical
392 properties (IOPs) in snow at the wavelengths relevant for photochemistry (UV). These
393 wavelength-dependent IOPs include the bulk extinction coefficient in snow ($Kext_{tot}$) and
394 the co-albedo of single scattering ($c\varpi_{eff}$); see Zatko et al. [2013] for more details about
395 the IOP calculations. $Kext_{tot}$ and $c\varpi_{eff}$, along with observations of downwelling surface
396 UV irradiance, solar zenith angle, cloud fraction, and soil albedo (0.1) [*Markvart et al*.,
397 2003, *Matthias et al*., 2000] are used to calculate 1-cm resolution vertical profiles of UV
398 actinic flux for each snowpit, following methods described in Zatko et al. [2013]. The
399 UV actinic flux profiles are used to calculate depth-dependent photolysis rate constants
400 for nitrate photolysis in snow as described below.

401

402 **2.2.2. Snow-Sourced Reactive Nitrogen Flux Calculations**

403 The modeled vertical profiles of actinic flux and observed snow nitrate concentrations are
404 used to calculate daily-average fluxes of snow-sourced N_r from each snowpit according
405 to E8.

$$F_{Nr}(z) = \int_{\lambda_0}^{\lambda_1} \sigma_{NO_3^-}(\lambda) \cdot \phi(T,pH) \cdot I(\lambda, z) \cdot [NO_3^-](z)\, d\lambda, \quad \text{E8}$$

$F_{Nr}(z)$ is the flux of snow-sourced N_r (molec cm^{-2} s^{-1}) at 1-cm depth (z) increments in the snow, σ_{NO3}^- is the wavelength (λ)-dependent absorption cross-section for nitrate photolysis (cm^2) from Berhanu et al. [2014], ϕ is the temperature- and pH-dependent quantum yield for nitrate photolysis (ϕ, molec $photon^{-1}$) from Chu and Anastasio [2003] (4.6×10^{-3} molec $photon^{-1}$ at T=267 K), I is the depth (z)- and λ-dependent actinic flux in the snow photic zone (photons cm^{-2} s^{-1} nm^{-1}), and $[NO_3^-](z)$ is the observed nitrate concentration (ng g^{-1}) in each snow layer. E8 is integrated over the UV wavelength region (λ=298-345 nm). The snow photic zone is defined as three times the e-folding depth of UV actinic flux in snow [*Zatko et al*., 2016]. The total flux of N_r to the boundary layer, F_{Nr}, is calculated according to E9.

$$F_{Nr} = \sum_{z_0}^{z_{3e}} F_{Nr}(z) \quad \text{E9}$$

Observed surface downwelling irradiance values for a solar zenith angle of 65°, the average SZA from mid-December to mid-February, are used for calculation of $I(\lambda,z)$ in E8. Therefore the calculated F_{Nr} values represent daily-averaged F_{Nr} values. It is assumed that all N_r escapes into the boundary layer due to its low solubility.

2.2.3. Snow Photochemistry Column Model (TRANSITS)

428 The flux of snow-sourced N_r from each snowpit is also calculated using a snow
429 photochemistry column model, TRansfer of Atmospheric Nitrate Stable Isotopes To the
430 Snow (TRANSITS) model [*Erbland et al*., 2015]. TRANSITS is a multilayer, one-
431 dimensional model that simulates nitrate photochemistry in the snow and allows for
432 chemical exchange between the air and snow and calculates the isotopic composition of
433 snow nitrate. The model was originally developed to simulate snow nitrate photolysis and
434 subsequent nitrogen recycling at the air-snow interface on the East Antarctic plateau
435 (Dome C), and has been adapted to mid-latitude, shallow-snowpack conditions for this
436 study. The model has a well-mixed, atmospheric boundary layer with a height of 50 m
437 and a snow compartment containing up to 50 1-cm thick layers. In the atmosphere and in
438 each snow layer, the model solves a general mass-balance equation for nitrate
439 concentration and isotopic composition [*Erbland et al*., 2015] at each time step (1 hour).
440
441 In TRANSITS, nitrate is deposited to the snow surface via dry deposition. Nitrate dry-
442 deposition is calculated using the campaign-averaged observed boundary layer mixing
443 ratios for HNO_3 (5784 ng m^{-3}) and NO_3^- (5777 ng m^{-3}) and an assumed dry-deposition
444 velocity of 0.03 cm s^{-1}, which is similar to the dry-deposition velocity used in Edwards et
445 al. [2013, 2014] (0.02 cm s^{-1}) (see Supplementary Table 1B for nitrate dry-deposition
446 fluxes). Nitrate diffuses through the snowpack based on a diffusion coefficient that is
447 dependent on temperature, pressure, snow specific surface area, snow density, and
448 tortuosity [*Crowley et al*., 2010, *Durham et al*., 1986, *Massmann*, 1998].
449

We include only the major channel for the production of N_r from nitrate photolysis (E1) in TRANSITS. The minor channels, E2-E5, all consist of chemistry of the intermediate in nitrate photolysis, nitrite, which will photolyze or react rapidly once produced to form N_r. We assume no export of snow-sourced N_r out of the atmospheric box, which is consistent with the low wind speeds and stable boundary layer conditions observed during the campaign. In this way there is no net loss of nitrate from the snow; however, vertical redistribution of snow nitrate can occur which would result in distinctive vertical profiles of nitrate concentration and $\delta^{15}N(NO_3^-)$ in the snow column. In addition to calculating the flux of snow-sourced N_r, TRANSITS calculates vertical profiles of nitrate concentration and isotopes ($\delta^{15}N(NO_3^-)$) in the snow. To calculate $\delta^{15}N(NO_3^-)$ in the snow, the nitrate photolysis fractionation factor ($^{15}\varepsilon_{pho}$) is calculated at each time step and is dependent upon the spectral distribution of the UV irradiance at the snow surface [*Bernhau et al*., 2014, *Erbland et al*., 2015]. Calculated $^{15}\varepsilon_{pho}$ values range from -88 to -35‰ between the snowpits and are constant with snow depth.

In this study, TRANSITS is run at hourly resolution and is spun up beginning 27 days before the start of the campaign using available atmospheric chemical (boundary layer gas-phase and aerosol-phase nitrate) and meteorological data (air temperature and pressure). A constant model boundary layer height of 50 m is assumed, which is a rough estimate of daily-averaged boundary layer heights based on sodar facsimile data from NOAA. The campaign-averaged observed boundary layer total nitrate (HNO_3+ NO_3^-) mixing ratio (11.56 μg m^{-3}) was used to spin up the model. We collected and measured atmospheric $\delta^{15}N(NO_3^-)$ throughout the campaign using a high volume air sampler with

Nylasorb filters. However, comparison with the aerosol nitrate (NO_3^-) concentration measurements from the PMEL two-stage, multi-jet cascade impactor measurements revealed incomplete trapping. Since non-quantitative collection of nitrate may influence the observed $\delta^{15}N(NO_3^-)$ values, the data was not used in this study. We instead use surface snow $\delta^{15}N(NO_3^-)$ observations to represent atmospheric $\delta^{15}N(NO_3^-)$ (Figure 1a). The TRANSITS snowpack is initialized by setting the snow height equal to 50 cm, the snow photic zone to 6 cm (average photic zone depth for all snowpits), and using the measured snow nitrate concentration and $\delta^{15}N(NO_3^-)$ vertical profiles from the first snowpit of the campaign (January 15). The snowfall event on January 31 is simulated in the model, but the other smaller events are not included. As the model evolves, "snapshots" of the top 25-cm of snow are taken on days corresponding to each snowpit and modeled profiles of nitrate concentration and $\delta^{15}N(NO_3^-)$ are compared to observed profiles for each snowpit. Since vertical profiles of snow $\delta^{15}N(NO_3^-)$ are highly sensitive to photochemical-driven redistribution of N_r in the snowpack [*Erbland et al.*, 2013, 2015], observed $\delta^{15}N(NO_3^-)$ provides a metric to assess model-calculated F_{Nr}.

Maria Zatko 7/11/16 9:01 PM
Deleted: HNO_3 +

3. Results and Discussion

3.1. Observations

3.1.1. Nitrate Concentrations and $\delta^{15}N(NO_3^-)$ in the Surface Snow

Figure 1a shows mean surface snow $\delta^{15}N(NO_3^-)$ values for each snowpit, which range from -5.5 to 11.1‰. The lowest observed surface snow $\delta^{15}N(NO_3^-)$ occurred immediately

497 after the only significant fresh snowfall event on Jan. 30 – 31 (-5.5‰). All other surface
498 snow samples were over 10‰ higher (5.2 to 11.1‰).
499
500 Figure 1b shows surface snow nitrate concentration measurements for each snowpit,
501 which range from 800 to 18,000 ng g^{-1}. Similar to $\delta^{15}N(NO_3^-)$, surface-snow nitrate
502 concentrations are lowest during the snowfall event on January 30 through January 31,
503 with the exception of February 11 when the snow was rapidly melting. Similarly,
504 boundary layer gas (HNO_3) and aerosol-phase (NO_3^-) nitrate mixing ratios decrease by a
505 factor of 6 between January 30 and January 31 (Supplementary Figure 1B) compared to
506 the rest of the field campaign. In addition to the gas and aerosol phase nitrate mixing
507 ratios presented in the Supplemental Material, Veres et al. [2015] also show decreases in
508 the daily-maximum HO_2NO_2 mixing ratios on January 30 and January 31 during
509 UBWOS2014. The decrease in HO_2NO_2 mixing ratios corresponds to a sharp decrease in
510 snow nitrite concentrations (see Figure 7 in Veres et al. [2015]).
511
512
513 Generally, the surface-snow $\delta^{15}N(NO_3^-)$ values fall within the range of primary
514 anthropogenic $\delta^{15}N$ values (4-25‰) [*Felix and Elliott*, 2014, *Walters et al*., 2015].
515 During snow events the boundary layer is less stable, possibly allowing for the transport
516 of nitrate from remote sources outside the basin. In unpolluted, mid-latitude
517 environments, background atmospheric $\delta^{15}N(NO_3^-)$ ranges from -6 to -2‰ [*Morin et al*.,
518 2009]. During the major snowfall event on January 30 - 31, surface-snow $\delta^{15}N$ values are
519 ~10‰ lower compared to the rest of the campaign, suggesting that nitrate from beyond

the basin deposits to the snow surface. Two-day NOAA HYSPLIT back trajectories [*Rolph*, 2016, *Stein et al*., 2015] show that the air mass on January 31 in the Uintah Basin originated in the Pacific Ocean, which is distinctly different from the other air masses that reached the Uintah Basin during UBWOS2014 (see Supplemental Material, Figures 4B-15B). Uintah Basin boundary layer air masses typically originated in the intermountain west region and often centered over eastern Utah for several days.

3.1.2. Snow Depth Profiles of Snow Optical Properties, Nitrate Concentrations, and $\delta^{15}N(NO_3^-)$

In this section and the following sections, we focus on three snowpits (January 22, January 31, February 4) as being representative of the time period before, during, and after the largest snow event. The other 9 snowpits will not be discussed in detail, but observed and modeled vertical profiles of chemical and optical measurements for all 12 snowpits can be found in Supplementary section A.

Figures 2a and 2b show vertical profiles of snow optical properties from an 18-cm deep snowpit dug on January 22, which represents typical profiles from the beginning of the field campaign until before the first snow event. Black carbon concentrations (C_{BC}, ng g^{-1}) range from 3 to 100 ng g^{-1} with the highest concentrations in the top several centimeters of snow. Below 3 cm snow depth, C_{BC} decreases dramatically. Figure 2b shows the average absorption Ångstrom exponent ($\mathring{A}$) from λ=450-600 nm. Over this wavelength range, the dominant absorber at the snow surface is non-BC material ($\mathring{A}$ is

543 nearly 5), and both BC and non-BC contribute to absorption in sub-surface snow layers
544 ($\AA$ ranges from 2 to 2.7). Although BC and non-BC material are both responsible for the
545 absorption of radiation at λ=450-600 nm, non-BC material is responsible for between
546 99.6 and 100% of UV (λ=300-350 nm) absorption at all depths in this and in all snowpits
547 measured during the field campaign. The top 3 cm of snow contains the highest
548 concentration of both BC and non-BC material; we define this layer as the "dusty layer"
549 and is represented as a brown shaded region in Figure 2.
550
551 Figures 2c and 2d show vertical profiles of snow optical properties from a 14-cm deep
552 snowpit dug on January 31. It snowed 5 cm between the afternoon of January 30 and
553 morning of January 31, and this new snow layer is evident in Figures 2c and 2d because
554 the dusty layer is now located roughly 5 cm below the snow surface. Figure 2c shows that
555 C_{BC} ranges from 5 to 100 ng g^{-1}; the maximum C_{BC} value has been buried deeper into the
556 snow. Figure 2d shows that $\AA$ is close to 1 at the snow surface, indicating that BC
557 material dominates visible absorption at the snow surface immediately following the
558 fresh snowfall event. Figures 2e and 2f show vertical profiles of snow optical properties
559 from a 24-cm deep snowpit dug on February 4, 5 days after the snow event. In this
560 snowpit, C_{BC} ranges from 4 to 100 ng g^{-1} and $\AA$ ranges from 1.7 to 3.4. Figures 2e and 2f
561 show that the original dusty layer is still located roughly 5 cm below the snow surface
562 and that a new dusty layer has formed at the snow surface.
563
564 Figures 3a-c shows observed vertical profiles of nitrate in snow from snowpits dug on
565 January 22, January 31, and February 4. Prior to the fresh snowfall event, snow nitrate

Maria Zatko 7/12/16 7:32 AM
Deleted: this layer

Maria Zatko 7/12/16 7:32 AM
Deleted: concentration and nitrogen isotopes ($\delta^{15}N(NO_3^-)$)

569 concentrations are highest at the surface (13,900 ng g^{-1}), and decrease exponentially in
570 the top 10 cm to a low of 90 ng g^{-1} at 18 cm depth (Figure 3a). Immediately following
571 the fresh snowfall event, the highest nitrate concentrations (12,200 ng g^{-1}) are buried
572 below 5 cm of fresh snow within the dusty layer at 5 – 7 cm depth. The measured nitrate
573 concentrations in the fresh snow layer range from 1,280 to 4,640 ng g^{-1}, which is up to 10
574 times lower than nitrate concentrations in the dusty layer (Figure 3b). Five days after the
575 fresh snowfall event, the highest nitrate concentrations are still located roughly 7 cm
576 below the snow surface within the dusty layer, but surface nitrate concentrations are a
577 factor of 2 higher compared to immediately after the fresh snowfall event (Figure 3c).
578
579 Figures 3d-f shows measured snow $\delta^{15}N(NO_3^-)$ in each of the snowpits, which ranges
580 from -5.5‰ to 13‰. In the Jan. 22 snowpit, measured $\delta^{15}N(NO_3^-)$ is highest near the top
581 and bottom of the snowpit and lowest from 12-cm to 16-cm depth (Figure 3d). Following
582 the fresh snowfall event on Jan. 30 – 31, snow $\delta^{15}N(NO_3^-)$ values are lightest at the snow
583 surface and increase with depth in the fresh snow layer until the top of the dusty layer,
584 below which they decrease to -3.5‰ (Figure 3e). Five days after the fresh snowfall event,
585 measured $\delta^{15}N(NO_3^-)$ is most enriched in the dusty layer and at the snow surface (Figure
586 3f).
587
588 The last snowfall event prior to the start of the campaign occurred on December 19 and
589 resulted in roughly 1 cm of snow accumulation (Supplementary Figure 5A). The high
590 concentrations of LAI and nitrate in surface snow on January 22, combined with the
591 prolonged lack of snowfall, suggest continual dry-deposition of LAI to the surface snow.

We speculate that the major source of LAI originates from truck traffic on the dirt roads in the area of the field site due to high values of $\mathring{A}$ (Figure 2). The factor of 150 and 17 decrease in nitrate and black carbon concentrations, respectively, from the surface to 18-cm depth on January 22 suggests that minimal nitrate and LAI are transported (via e.g., diffusion or meltwater transport) from upper to lower snow layers. Immediately after the snowfall event on January 31, nitrate and black carbon concentrations are 10 and 3 times lower, respectively, in the surface snow layers compared to earlier in January, because the fresh snow has lower concentrations of these species. Even just five days after the snowfall event on January 30 - 31, concentrations of nitrate and the Ångstrom exponent ($\mathring{A}$) in the snow surface layer have increased by a factor of 2, likely due to dry deposition of these species to the surface in the absence of snowfall.

The $\delta^{15}N(NO_3^-)$ profiles in snow do not immediately suggest significant photolysis-driven redistribution of nitrate in the snowpack, which would result in the lightest values at the surface, increasing exponentially with depth as observed in Antarctica [*Erbland et al*., 2013]. Prior to the first snowfall event on January 30-31, the surface dusty layer contains the highest values of measured $\delta^{15}N(NO_3^-)$, which are similar to that expected from primary emission of NO_x from anthropogenic sources [*Felix and Elliott*, 2014, *Walters et al*., 2015]. We speculate that the depleted $\delta^{15}N(NO_3^-)$ values towards the bottom of the snowpit correspond to remote-sourced atmospheric nitrate that was deposited during the large snow event (~20 cm of snow) on December 4. Emissions of microbial NO from subniveal soil could also lead to depleted $\delta^{15}N(NO_3^-)$ if this NO is oxidized to nitrate in the snowpack and deposited to the surface of snow grains before

escaping to the atmosphere. However, the depleted $\delta^{15}N(NO_3^-)$ would also likely correspond with enhanced nitrate concentrations, which is not observed (Figures 3a-c). Additionally, calculations by Zatko et al. [2013] suggest that the lifetime of NO_x against oxidation to HNO_3 in snow interstitial air is long enough so that most NO emitted from soil microbial activity would likely be transported to the atmospheric boundary layer prior to oxidation. On January 31, depleted $\delta^{15}N(NO_3^-)$ measurements at the snow surface suggest that there is deposition of nitrate from less polluted regions surrounding the basin during the snow event. The increase in surface snow $\delta^{15}N(NO_3^-)$ values after January 31 is likely due to deposition of primary-sourced nitrate from anthropogenic NO_x sources in the basin. In the following section, we examine the influence of photolysis of snow nitrate on the profiles of $\delta^{15}N(NO_3^-)$ in snow.

3.2. Calculations

3.2.1. Calculations of Snow Actinic Flux Profiles and Flux of Snow-Sourced N_r

Figure 4a-c show calculated vertical profiles of UV actinic flux normalized to surface downwelling irradiance for the three snowpits. On January 22, the normalized actinic flux ratio is nearly 4 at the snow surface because actinic flux is calculated by integrating irradiance over a sphere (surface area of $4\pi r^2$) and also because scattering in snow dominates over absorption. In Figure 4a, the actinic flux decreases to 2.9 within the top centimeter of snow due mainly to UV absorption by non-BC in the surface snow layer. The actinic flux is rapidly extinguished in the dusty layer and continues to decrease with increasing depth in the snow, reaching a value of 0.01 at 18-cm depth. The blue shaded

Maria Zatko 8/10/16 7:24 AM
Deleted: s

Maria Zatko 7/12/16 7:35 AM
Deleted: The non-normalized actinic flux values and surface downwelling irradiance values for all snowpits are presented in the supplementary material.

region represents the snow photic zone (top 5 cm of snow) on January 22. The snow photic zones calculated in this study (4-7 cm) are much shallower compared to calculated snow photic zones in polar regions (72-207 cm in Antarctica, 6-51 cm in Greenland) [*Zatko et al.*, 2016] because UV absorption by LAI in the snow photic zone are at least five orders of magnitude higher in Utah compared to Antarctica and Greenland.

In the snowpits following the fresh snowfall event, the existence of the dusty layer deeper into the snow influences the vertical actinic flux profile and increases the photic zone depth from 5 to 7 cm. The fresh snow at the surface contains less LAI compared to the dusty layer, therefore actinic flux values are higher in the top several centimeters of snow compared to actinic flux values measured before the snowfall event even though r_e values in the new snow are a factor of 3.3-8.3 times smaller than the underlying depth hoar grains. Smaller r_e values lead to more scattering in the snow, which increases the probability of absorption by LAI. Although actinic flux values are highest at the surface on January 31, Figure 4b illustrates that UV radiation is rapidly attenuated below the fresh snow layer because radiation is forward-scattered into the highly-absorbing dusty layer. As a result, there is roughly an order of magnitude less actinic flux at 14-cm depth on January 31 compared to January 22.

The presence of a new dusty layer on the snow surface five days after the fresh snowfall event does not significantly alter the vertical profile of normalized UV actinic flux likely because UV absorption by LAI in the surface layer is at least 5 times lower than UV absorption by LAI in the original dusty layer (surface snow from January 22 snowpit).

Surface snow UV albedo is strongly influenced by the presence of LAI, and Supplemental Figure 2B shows that snow UV albedo is lowest right before the snowfall event on January 30-31 and highest immediately afterwards.

We use these actinic flux profiles and the observed snow nitrate concentrations (Figure 3a-c) to calculate daily-averaged fluxes of snow-sourced N_r (molec cm^{-2} s^{-1}) at 1-cm depth (z) increments in the snow ($F_{Nr}(z)$) and total fluxes of N_r to the boundary layer (F_{Nr}) according to E8 and E9 for each of the three snowpits (Figure 4d-f). Prior to the fresh snowfall event, $F_{Nr}(z)$ decreases exponentially with depth in the photic zone. $F_{Nr}(z)$ is highest at the snow surface because that is where both actinic flux and snow nitrate concentrations are highest. Daily-average F_{Nr} summed over the snow photic zone is 5.6×10^8 molec cm^{-2} s^{-1} on January 22 (Figure 4d and Table 1). Immediately following the fresh snowfall event, $F_{Nr}(z)$ decreases by a factor of 3 at the surface because of the factor of 4 decrease in surface snow nitrate concentrations, which is partially compensated by the higher UV actinic flux in the top of the snow photic zone (Figure 4b). The daily-averaged F_{Nr} on January 31 is 1.9×10^8 molec cm^{-2} s^{-1}, which is a factor of 3 lower than total F_{Nr} on January 22. Five days later, $F_{Nr}(z)$ has increased by a factor of 2 at the surface due to the factor of 2 increase in surface nitrate concentrations (Figure 3c and 4f). The daily-averaged F_{Nr} on February 4 is 3.2×10^8 molec cm^{-2} s^{-1}, which is a factor of 1.7 higher than total F_{Nr} on January 31.

Maria Zatko 8/9/16 8:03 AM
Deleted: (Figure 4)

Maria Zatko 8/9/16 8:03 AM
Deleted: (Figure 5a)

Maria Zatko 7/12/16 7:36 AM
Deleted: near the snow surface.

Maria Zatko 8/9/16 8:02 AM
Deleted: 5a

Maria Zatko 8/10/16 7:26 AM
Deleted: 5

Maria Zatko 8/10/16 7:26 AM
Deleted: c

3.2.2. Snow Photochemistry Column Model

694 The snow chemistry column model is used to calculate the time-dependent flux of snow-
695 sourced N_r (F_{Nr}) and the depth profile of nitrate concentration and $\delta^{15}N(NO_3^-)$. Figure 5
696 shows the diurnal F_{Nr} values on January 22, January 31, and February 4. The daily-
697 averaged snow F_{Nr} on January 22 is 6.3×10^8 molec cm^{-2} s^{-1}. Immediately following the
698 snow event, the daily-averaged snow F_{Nr} decreases by a factor of 11 compared to January
699 22 (5.6×10^7 molec cm^{-2} s^{-1}). The dramatic difference in F_{Nr} is due to the differences in
700 nitrate concentrations in the top several centimeters of snow. Modeled snow nitrate
701 concentrations in the fresh snow layer on January 31 are between 30 and 300 times lower
702 compared to nitrate concentrations in the dusty layer. Five days after the snow event, the
703 daily-averaged snow F_{Nr} has increased by a factor of 2 (1.2×10^8 molec cm^{-2} s^{-1}) because
704 deposition of nitrate to the snow surface layer enhances surface nitrate concentrations and
705 thus F_{Nr}. Calculated daily average F_{Nr} using observed (section 3.2.1) and modeled
706 (TRANSITS) snow nitrate concentrations agree within a factor of ~2 (Table 1); modeled
707 F_{Nr} tends to be lower because modeled snow nitrate concentrations are lower than
708 observed (Figure 3).
709
710 Figure 6 shows hourly F_{Nr} values calculated for the entire UBWOS2014 campaign using
711 TRANSITS. From the start of the campaign until the fresh snow event on January 31, the
712 daily maximum F_{Nr} values increase as surface snow nitrate concentrations increase due to
713 continual dry-deposition of atmospheric nitrate to the snow surface. Immediately after the
714 snow event on January 31, daily maximum F_{Nr} values are lowered by more than a factor
715 of 10 due to decreased nitrate concentrations in the snow photic zone. Following the
716 snow event, the flux of snow-sourced N_r gradually increases again due to dry-deposition

Maria Zatko 8/10/16 7:27 AM
Deleted: 6

Maria Zatko 8/10/16 7:27 AM
Deleted: 8

Maria Zatko 8/10/16 7:28 AM
Deleted: 7

of nitrate to the surface layer, although daily maximum F_{Nr} values remain lower compared to values before the snow event throughout the remainder of the field campaign.

Figure 3 shows modeled snow nitrate concentrations and $\delta^{15}N(NO_3^-)$ from TRANSITS compared to the observations. The general shapes of the modeled and measured vertical profiles of nitrate concentration are in agreement for all three snowpits; both modeled and measured nitrate concentrations are highest in the dusty layer and lowest near the bottom of the snowpit (Figure 3a-c). Both the model and the observations show increased snow nitrate concentrations at the surface following the fresh snowfall event, but the model tends to underestimate surface snow nitrate concentrations after the snow event.

Modeled $\delta^{15}N(NO_3^-)$ is also within the range of observations (Figure 3d-f). Modeled $\delta^{15}N(NO_3^-)$ at the top surface snow layer becomes more depleted from the January 22 to the January 31 snowpit reflecting the decrease in atmospheric $\delta^{15}N(NO_3^-)$ in the model based on surface snow observations (Figure 1a). Without additional snowfall between January 31 and February 4, surface snow $\delta^{15}N(NO_3^-)$ becomes more enriched in the model over this time period because model atmospheric $\delta^{15}N(NO_3^-)$ becomes more enriched (Figure 1a). In contrast, the observations retain this light $\delta^{15}N(NO_3^-)$ at a depth of ~2 cm until the February 11 snowpit (see supplement A). The difference between modeled and observed $\delta^{15}N(NO_3^-)$ at 2 cm depth after January 31 may be due to the redistribution of surface snow by wind, and the fact that each snowpit was dug in a slightly different location. Blowing snow will bury the surface snow with light

Maria Zatko 7/12/16 7:37 AM
Deleted: Observed snow nitrate concentration and $\delta^{15}N(NO_3^-)$ values are used to assess results from TRANSITS. $\delta^{15}N(NO_3^-)$ observations are particularly useful as a metric to assess the F_{Nr} values calculated in TRANSITS because $\delta^{15}N(NO_3^-)$ vertical profiles are highly sensitive to photolytic recycling and photolysis-driven loss of nitrate from snow.

Maria Zatko 8/10/16 7:28 AM
Deleted: 8

Maria Zatko 8/10/16 7:28 AM
Deleted: 8a-c

Maria Zatko 8/10/16 7:30 AM
Deleted: 8

$\delta^{15}N(NO_3^-)$, and subsequent atmospheric deposition of more enriched $\delta^{15}N(NO_3^-)$ will occur onto this new, wind-blown snow surface, retaining the light $\delta^{15}N(NO_3^-)$ at 2 cm depth. In contrast to the observations, the model does not account for windblown redistribution of snow, and calculates the time-evolution of nitrate concentration and $\delta^{15}N(NO_3^-)$ gradients of a single snowpit.

To examine the sensitivity of snow nitrate to photolysis, we turn off photolysis of snow nitrate in the model by setting $\phi = 0$. When snow nitrate photolysis is turned off, snow nitrate concentrations change by less than 0.5% in all snowpits, resulting in relatively little sensitivity of modeled snow nitrate concentration to snow photochemistry because only this small fraction (< 0.5%) of nitrate is lost via photolysis at all depths. Despite the large nitrogen isotope fractionation (ε = -88 to -35‰) resulting from the photolysis of snow nitrate, the difference in modeled $\delta^{15}N(NO_3^-)$ when snow nitrate is turned on ($\phi = 4.6 \times 10^{-3}$) and off ($\phi = 0$) is small because of the very small fraction of nitrate photolyzed.

In another sensitivity study, we calculate the maximum possible F_{Nr} in the Uintah Basin by increasing the value of ϕ until modeled snow $\delta^{15}N(NO_3^-)$ falls outside the full range of observations. Above $\phi = 0.2$, there is significant disagreement (when the maximum change in $\delta^{15}N(NO_3^-)$ is > 1σ of the mean $\delta^{15}N(NO_3^-)$ in all snowpits) between modeled and measured $\delta^{15}N(NO_3^-)$ values. Using $\phi = 0.2$ results in more enriched $\delta^{15}N(NO_3^-)$ at depth due to enhanced photolytic loss, and more depleted $\delta^{15}N(NO_3^-)$ at the snow surface due to the deposition of isotopically light snow-sourced nitrate. Using $\phi = 0.2$ results in a

Maria Zatko 7/12/16 7:38 AM

Deleted: As discussed in the introduction, laboratory-based quantum yield measurements range from 0.003 to 0.6 [*Chu and Anastasio*, 2003, *Meusinger et al.*, 2014, *Zhu et al.*, 2010]. We use ϕ from Chu and Anastasio (4.6×10^{-3} at T=267 K, which is the average daytime temperature during the campaign) in our base case simulation discussed above as it results in calculated values of F_{Nr} in Antarctica and Greenland that are the same order of magnitude as observations [*Zatko et al.*, 2016]. In a sensitivity study,

Maria Zatko 7/12/16 7:39 AM

Deleted: When photolysis is turned on, snow $\delta^{15}N$ values are slightly lower in the top several centimeters due to deposition of isotopically light, snow-sourced nitrate and $\delta^{15}N$ values are slightly more enriched at depth. On January 22, the $\delta^{15}N(NO_3^-)$ profiles in the snow photic zone with and without snow nitrate photolysis ≤ 0.1‰ , on January 31 by ≤ 1.3‰, and on February 4 by ≤ 0.3‰. Snow nitrate photolysis influences both the magnitude and gradient of the snow $\delta^{15}N(NO_3^-)$ profiles on January 31 and February 4 more than January 22, likely because light-absorbing concentrations are lower in the fresh snow layer.

maximum possible F_{Nr} at least 45 times larger than when using ϕ = 4.6x10^{-3} for all snowpits (see Table 1).

4. Impact of Snow-Sourced N_r on the Boundary Layer Reactive Nitrogen Budget

4.1. NO_x

We first assume that all N_r is NO_x and use F_{Nr} values calculated using the snow photochemistry column model to estimate the impact of F_{NOx} on the NO_x budget in the Uintah Basin. Using the best estimate for the quantum yield of nitrate photolysis (ϕ=4.6x10^{-3}), the modeled daily-averaged flux of snow-sourced NO_x ranges from 5.6x10^{7} to 7.2x10^{8} molec cm^{-2} s^{-1} and the maximum F_{Nr} value is 3.1x10^{9} molec cm^{-2} s^{-1} for the entire campaign (Supplementary Table 4B). The top-down NO_x emission inventory for oil, gas, and all other sources excluding the Bonanza power plant in Duchesne and Uintah counties is 6.5x10^{6} kg NO_x yr^{-1} [*Ahmandov et al.*, 2015]. The power plant is excluded because its emissions occur above the boundary layer due to the plume's positive buoyancy. Assuming a constant NO_x emission rate and using the area of Duchesne (8433 km^2) and Uintah counties (11658 km^2), the top-down NO_x emission estimate for the Uintah and Duchesne counties is 1.2x10^{12} molec cm^{-2} s^{-1}. The emission of primary NO_x in these two counties is thus at least 300 times higher than the estimated snow NO_x emissions, implying that snow-sourced NO_x fluxes likely do not influence the NO_x boundary layer budget in the highly-polluted Uintah Basin. If the upper limit of ϕ = 0.2 is used, snow-sourced NO_x emissions are still at least 7 times smaller than primary NO_x

Maria Zatko 7/12/16 7:40 AM
Deleted: reactive nitrogen

emissions. Although reactive nitrogen is likely being emitted from the snow into the boundary layer, the snow-sourced NO_x signal is swamped by emissions from primary anthropogenic sources in the Uintah Basin.

4.2. HONO

Only the major channel for snow nitrate photolysis (E1) is simulated in the TRANSITS model, although nitrate can also photolyze via E2 and form both NO_x and HONO (E3-E5). The surface snow pH ranged from 2-4 during the campaign (see Figure 3A in Supplemental Material), which is low enough to enable direct volatilization of HONO from the snow. We estimate the maximum possible influence of the snow-photolytic source of boundary layer HONO by assuming that all snow-sourced N_r is in the form of HONO. If we assume that the campaign-maximum F_{Nr} value (3.1×10^9 molec cm^{-2} s^{-1}) is all HONO that escapes from the snow into the boundary layer, a boundary layer height of 50 m, and a lifetime of HONO of 18 minutes (at solar noon) [*Edwards et al.*, 2013], snow nitrate photolysis would contribute a maximum of 25 pptv of HONO to the boundary layer at solar noon. The modeled and observed Uintah Basin boundary layer HONO mixing ratios presented in Edwards et al. [2014] range from ~20 pptv at night to up to 150 pptv during the day, which suggests that the daytime fluxes of reactive nitrogen are not a significant source of HONO to the boundary layer compared to other HONO sources in the basin. Our estimated maximum HONO flux is comparable to snow-sourced HONO fluxes measured at another polluted, mid-latitude location (Paris, France), estimates of which ranged from $0.7\text{-}3.1 \times 10^{10}$ molec cm^{-2} s^{-1} (assuming a snow density of 0.36 g cm^{-3} and snow photic zone depth of 6 cm) [*Michoud et al.*, 2015]. If the upper

Maria Zatko 8/4/16 8:15 AM
Deleted: snow-sourced N_r for

Maria Zatko 8/4/16 8:15 AM
Deleted: mixing ratios

853 limit of ϕ = 0.2 is used (campaign-maximum F_{Nr}=1.4x10^{11} molec cm^{-2} s^{-1}), the maximum
854 boundary layer HONO mixing ratio calculated using this approach is 1.1 ppbv at solar
855 noon, which would significantly impact boundary layer HONO mixing ratios in the
856 Uintah Basin. Given that HONO is thought to be only a minor fraction of total N_r emitted
857 from snow [*Beine et al*., 2008], we consider this to be an overestimate.
858
859 **5. Conclusions**
860 This study estimates the influence of snow nitrate photolysis on the boundary layer
861 reactive nitrogen (N_r) budget in the Uintah Basin, which is a region with heavy oil and
862 natural gas extraction processes. Observations of snow optical properties, including
863 ultraviolet (UV) light-absorbing impurities (e.g., black carbon, dust, organics), radiation
864 equivalent ice grain radii, and snow density from 12 snowpits measured during the
865 Uintah Basin Winter Ozone Study (UBWOS) 2014 are incorporated into a snowpack
866 radiative transfer model to calculate vertical profiles of UV actinic flux in 12 snowpits
867 dug during the campaign. The calculated UV actinic flux profiles along with
868 measurements of nitrate concentration are used to calculate snow-sourced N_r fluxes
869 associated with snow nitrate photolysis using both a simple equation (E8) and a more
870 complex snow photochemistry column model, which yield similar results. Snow nitrate
871 photolysis in the column model is constrained by 1-cm depth resolved observations of
872 $\delta^{15}N(NO_3^-)$ in the snowpits, which is highly sensitive to UV photolysis [*Erbland et al*.,
873 2015].
874

Maria Zatko 7/12/16 7:41 AM
Deleted: at 1-cm depth intervals

Maria Zatko 7/12/16 7:41 AM
Deleted: vertical

Maria Zatko 7/12/16 7:41 AM
Deleted: reactive nitrogen (

Maria Zatko 7/12/16 7:41 AM
Deleted:)

Maria Zatko 7/12/16 7:42 AM
Deleted: .
The snow-sourced N_r fluxes calculated using calculated using calculated UV actinic flux profiles and observed snow nitrate concentrations are similar in magnitude to the daily-averaged fluxes of snow-sourced N_r calculated using the more complex snow photochemistry column model.

The daily-averaged flux snow-sourced N_r (F_{Nr}) to the boundary layer ranges from $5.6x10^7$ to $7.2x10^8$ molec cm^{-2} s^{-1} and the modeled campaign-maximum F_{Nr} is $3.1x10^9$ molec cm^{-2} s^{-1}. The top-down emission estimate of primary NO_x in the Uintah and Duchesne counties reported in Ahmadov et al. [2015] is at least 300 times higher than estimated snow NO_x emissions, assuming that all N_r is emitted as NO_x. This suggests that snow-sourced NO_x fluxes likely have little influence on the boundary layer NO_x budget in the highly-polluted Uintah Basin. Assuming that all N_r is emitted as HONO also suggests that the snow-sourced reactive nitrogen fluxes associated with snow nitrate photolysis do not significantly contribute to boundary layer HONO mixing ratios in the Uintah Basin. The relative importance of the flux of NO_x and HONO will influence the impact of the recycling of N_r in snow on the chemistry of the boundary layer in snow-covered regions, but is unknown. Knowledge of the chemical speciation of snow-source N_r is required for a better understanding of the full impact of snow on local oxidant budgets. However, in the Uintah Basin, we conclude that air quality models can safely neglect the recycling of reactive nitrogen in snow when identifying the most effective strategies for reducing wintertime ozone abundances.

Maria Zatko 7/12/16 7:45 AM
Deleted: The snow-sourced N_r fluxes calculated using calculated UV actinic flux profiles and observed snow nitrate concentrations are similar in magnitude to the daily-averaged fluxes of snow-sourced N_r calculated using the more complex snow photochemistry column model.

Maria Zatko 7/12/16 7:45 AM
Deleted: Snow-sourced NO_x fluxes are highly dependent on nitrate concentrations in the top several centimeters of snow; F_{Nr} values are roughly an order of magnitude higher in snowpits with a surface dusty layer compared to a buried dusty layer.

Maria Zatko 7/12/16 7:46 AM
Deleted: also likely

Maria Zatko 7/12/16 7:46 AM
Deleted: reactive nitrogen

Acknowledgements

We gratefully acknowledge support from 155 backers from www.experiment.com, NSF PLR 1244817, PMEL contribution number 4468, and an EPA STAR fellowship to M.C. Zatko. The Uintah Basin Winter Ozone Studies were a collaborative project led and coordinated by the Utah Department of Environmental Quality (UDEQ) with support from the Uintah Impact Mitigation Special Service District (UIMSSD), the Bureau of

Land Management (BLM), the Environmental Protection Agency (EPA), and Utah State University. The authors acknowledge the NOAA/ESRL Chemical Sciences Division and Questar Energy Products for site preparation and support. We thank Kristen Shultz, Jim Johnson, Drew Hamilton, and Derek Coffman for all of their help before, during, and after the field campaign. We would also like to thank Dean Hegg for advice on aerosol sampling, Angela Hong and Jennifer Murphy for helpful discussions about NO_y vertical gradients, and Chad Mangum for laboratory assistance at USU. We thank Sarah Doherty for the use of the ISSW spectrophotometer and Stephen Warren for graciously allowing M.C. Zatko to borrow snow sampling instruments and gear and providing comments about this work. We thank Jonathan Raff for helpful discussions about soil microbial activity as well as Joost de Gouw and Gail Tonnesen for useful discussions about boundary layer HONO. Finally, we thank Lyatt Jaeglé, Joel Thornton, and Thomas Grenfell for their helpful comments. Joel Savarino and Joseph Erbland have been partly supported by a grant from Labex OSUG@2020 (Investissements d'avenir – ANR10 LABX56) during the development of the TRANSITS model.

References

Ahmadov, R., McKeen, S., Trainer, M., Banta, R., Brewer, A., Brown, S., Edwards, P.M., de Gouw, J.A., Frost, G.J., Gilman, J., Helmig, D., Johnson, B., Karion, A., Koss, A., Langford, A., Lerner, B., Olson, J., Oltmans, S., Peischl, J., Petron, G., Pichugina, Y., Roberts, J.M., Ryerson, T., Schnell, R., Senff, C., Sweeney, C., Thompson, C., Veres, P.R., Warneke, C., Wild, R., Williams, E.J., Yuan, B., Zamora, R.: Understanding high wintertime O3 pollution events in an oil- and natural gas-producing region of the western US. *Atmos. Chem. Phys*., 15, 411-429, doi:10.5194/acp-15-411-2015, 2015.

Anastasio, C. and Chu, L.: Photochemistry of nitrous acid (HONO) and nitrous acidium ion (H_2ONO^+) in aqueous solution and ice. *Environ. Sci. Tech*., 43, 1108-1114, 2009.

Beine, H., Colussi, A.J., Amoroso, A., Esposito, G., Montagnoli, M., Hoffman, M.R.: HONO emissions from snow. *Environ. Res. Lett*., 3, 045005, 6, 2008.

Berhanu, T.A., Meusinger, C., Erbland, J., Jost, R., Bhattcharya, S. K., Johnson, M. S., Savarino, J.: Laboratory study of nitrate photolysis in Antarctic snow. II. Isotopic effects and wavelength dependence. J. Chem. Phys., 140, 244306, doi:10.1063/1.4882899, 2014.

Carter, W. P. L., Seinfeld. J.H.: Winter O3 formation and VOC incremental reactivities in the Upper Green River Basin of Wyoming. Atmos. Environ., 50, 255-266, doi:10.1016/j.atmosenv.2011.12.025, 2012.

Casciotti, K.L., Sigman, D.M., Hastings, M., Bohlke, J.K., Hilkert, A.: Measurement of the oxygen isotopic composition of nitrate in seawater and freshwater using the denitrifier method. *Anal. Chem*., 74, 4905-4912, 2002.

Chu, L., and Anastasio. C.: Quantum Yields of Hydroxyl Radicals and Nitrogen Dioxide from the Photolysis of Nitrate on Ice. *J. Phys. Chem*., 107, 9594-9602, 2003.

Crowley, J.N., Ammann, M., Cox, R.A., Hynes, R.G., Jenkin, M.E., Mellouki, A., Rossi, M.J., Troe, J., Wallington, T.J.: Evaluated kinetic and photochemical data for atmospheric chemistry: Volume V – heterogeneous reactions on solid surfaces. Atmos. Chem. Phys., 10, 9059-9223, doi:10.5194/acp-10-9059-2010, 2010.

Delmas, R., Serca, D., Jambert, C.: Global inventory of NO_x sources. *Nutr. Cycl. Agroecosys*., 48, 51-60, 1997.

Doherty, S. J., Warren, S. G., Grenfell, T. C., Clarke, A. D., and Brandt, R. E.: Light-absorbing impurities in Arctic snow. *Atmos. Chem. Phys*., 10, 11647-11680, doi:10.5194/acp-10-11647-2010, 2010.

Domine, F., Bock, J., Voisin, D., Donaldson, D. J.: Can we model snow photochemistry? Problems with the current approaches. *J. Phys. Chem. A*, 117, 4733-4749, doi: 10.1021/jp3123314 2013.

Durham, J.L., Stockburger, L.: Nitric acid-air diffusion coefficient: Experimental determination. *Atmos. Environ*., 20(3), 559-563, 1986.

Edwards, P.M., Young, C.J., Aikin, K., de Gouw, J., Dube, W., Geiger, P., Gilman, J., Helmig, D., Holloway, J.S., Kercher, J., Lerner, B., Martin, R., McLaren, R., Parrish, D.D., Peischl, J., Roberts, J.M., Ryerson, T.N., Thornton, J., Warneke, C., Williams, E.J., Brown, S.S.: O3 photochemistry in an oil and natural gas extraction region during winter: simulations of a snow-free season in the Uintah Basin, Utah. *Atmos. Chem. Phys*., 13, 8955-8971, doi:10.5194/acp-13-8955-2013, 2013.

Edwards, P.M., Brown, S., Roberts, J., Ahmadov, R., Banta, R., de Gouw, J., Dube, W., Field, R., Flynn, J., Gilman, J., Graus, M., Helmig, D., Koss, A., Langford, A., Lefer, B., Lerner, B., Li, R., Li, S., McKeen, S., Murphy, S., Parrish, D., Senff, C., Soltis, J., Stutz, J., Sweeney, C., Thompson, C., Trainer, M., Tsai, C., Veres, P., Washenfelder, R., Warneke, C., Wild, R., Young, C., Yuan, B., Zamora, R.: High O3 pollution from carbonyl photolysis in an oil and gas basin. *Nature*, 514, 351-354, doi:10.1038/nature13767, 2014.

Erbland, J., Savarino, J., Morin, S., France, J.L., Frey, M.M., King, M.D.: Air-snow transfer of nitrate on the East Antarctic plateau – Part 2: An isotopic model for the interpretation of deep ice-core records. *Atmos. Chem. Phys.*, 15, 12079-12113, doi:10.5194/acpd-15-12079-2015, 2015.

Felix, J.D., Elliott, E.M., Shaw, S.L: Nitrogen isotopic composition of coal-fired power plant NO_x: Influence of emissions controls and implications for global emission inventories. *Env. Sci. Tech*., 46, 3528-3535, 2012.

Felix, J.D., Elliot, E.M.: Isotopic composition of passively collected nitrogen dioxide emissions: Vehicle, soil and livestock source signatures. *Atmos. Environ*., 92, 359-366, doi:10.1016/j.atmosenv.2014.04.005, 2014.

Field, R.A., Soltis, J., McCarthy, M.C., Murphy, S., Montague, D.C.: Influence of oil and gas field operations on spatial and temporal distributions of atmospheric non-methane hydrocarbons and their effect on O3 formation in winter. *Atmos. Chem. Phys*., 15, 3527-3542, doi:10.5194/acp-15-3527-2015, 2015.

Frey, M. M., Savarino, J., Morin, S., Erbland, J., and Martins, J. M. F.: Photolysis imprint in the nitrate stable isotope signal in snow and atmosphere of East Antarctica and implications for reactive nitrogen cycling. *Atmos. Chem. Phys*., 9, 8681-8696, 2009.

Freyer, H.D., Kley, D., Volz-Thomas, A., Kobel, K.: On the interaction of isotopic exchange processes with photochemical reactions in atmospheric oxides of nitrogen. *J. Geophys. Res*., 98, D8, 14791-14786, doi: 10.1029/93JD00874, 1993.

Gilman, J.B., Lerner, B.M., Kuster, W.C., de Gouw, J.A.: Source signature of volatile organic compounds from oil and natural gas operations in northeastern Colorado. *Environ. Sci. Technol.*, 47, 1297-1305, doi:10.1021/es304119a, 2013.

Grannas, A. M., Jones, A. E., Dibb, J., Ammann, M., Anastasio, C., Beine, H. J., Bergin, M., Bottenheim, J., Boxe, C. S., Carver, G., Chen, G., Crawford, J. H., Domine, F., Frey, M. M., Guzman, M. I., Heard, D. E., Helmig, D., Hoffman, M. R., Honrath, R. E., Huey, L. G., Hutterli, M., Jacobi, H. W., Klan, P., Lefer, B., McConnell, J., Plane, J., Sander, R., Savarino, J., Shepson, P. B., Simpson, W. R., Sodeau, J. R., von Glasow, R., Weller, R., Wolff, E. W., Zhu, T.: An overview of snow photochemistry: evidence, mechanisms and impacts. *Atmos. Chem. Phys.*, 7, 4329-4373, 2007.

Grenfell, T. C.: A Radiative Transfer Model for Sea Ice With Vertical Structure Variations. *J. Geophys. Res.*, 96, 16991-17001, 1991.

Grenfell, T.C., Warren, S.G.: Representation of a nonspherical ice particle by a collection of independent spheres for scattering and absorption of radiation. *J. Geophys. Res.*, 104(D24), 31697-31709, 1999.

Grenfell, T.C., Doherty, S.J., Clarke, A.D., Warren, S.G.: Light absorption from particulate impurities in snow and ice determined by spectrophotometric analysis of filters. Appl. Opt., 50(8), 2037-2048, doi:10.1364/AO.50.002037, 2011.

Guenther, A., Hewitt, N.C., Erickson, D., Fall, R., Geron, C., Graedel, T., Harley, P., Klinger, L., Lerdau, M., McKay, W.A., Pierce, T., Scholes, B., Steinbrecher, R., Tallamraju, R., Taylor, J., Zimmerman, P.: A global model of natural volatile organic compound emissions. *J. Geophys. Res.*, 100(D5), 8873-8892, 1995.

Hansen, J.E., Travis, L.D.: Light scattering in planetary atmospheres. *Space. Sci. Rev.*, 16, 527-610, 1974.

Heaton, T. H. E., Spiro, B., Robertson, M.C., *Oecologia*, 109, 4, 600-607, 1997.

Helmig, D., Thompson, C.R., Evans, J., Boylan, P., Hueber, J., Park, J.H.: Highly elevated atmospheric levels of volatile organic compounds in the Uintah Basin, Utah. *Environ. Sci. Technol.*, 48, 4707-4715, doi:10.1021/es405046r, 2014.

Honrath, R.E., Guo, S., Peterson, M.C., Dziobak, M.P., Dibb, J.E., Arsenault, M.A.: Photochemical production of gas phase NO_x from ice crystal NO_3^-. *J. Geophys. Res.*, 105(D19), 24183-24190, 2000.

Kaiser, J., Hastings, M.G., Houlton, B.Z., Rockmann, T., Sigman, D.M.: Triple oxygen isotope analysis of nitrate using the denitrifier method and thermal decomposition of N_2O. *Anal. Chem.*, 79, 599-607, doi:10.1021/ac061022s, 2007.

Maria Zatko 8/10/16 7:42 AM
Deleted: . ... [2]

Logan, J.A., Nitrogen oxides in the troposphere: Global and regional budgets. *J. Geophys. Res*., 88(C15), 10785-10807, doi:10.1029/JC088iC15p10785, 1983.

Mack, J., and Bolton, J. R.: Photochemistry of nitrite and nitrate in aqueous solution: A review. *J. Photochem. Photobiol*. A., 128, 1-13, 1999.

Martin, R., Moore, K., Mansfield, M., Hill, S., Harper, K., Shorthill, H.: Final report: Uintah Basin winter O3 and air quality study, December 2010 – March 2011. Energy Dynamics Laboratory, document number: EDL/11-039, 2011.

Massman, W.J. A review of the molecular diffusivities of H_2O, CO_2, CH_3, CO, O_3, SO_2, NH_3, N_2O, NO, and NO_2 in air, O_2 and N_2 near STP. *Atmos. Environ*., 32(6), 1111-1127, doi:10.1016/S1352-230(97)00391-9, 1998.

Markvart, T., Castalzer, L.: Practical handbook of photovoltaics: fundamentals and applications. Elsevier. ISBN 1-85617-390-9, 2003.

Matthias, A.D., Fimbres, A., Sano, E.E., Post, D.F., Accioly, L., Batchily, A.K., Ferreira, L.G.: Surface roughness effects on soil albedo. *Soil Sci. Soc. Am*. J., 64, 1035-1041, 2000.

Meusinger, C., Berhanu, T.A., Erbland, J., Savarino, J., Johnson, M.S.: Laboratory study of nitrate photolysis in Antarctic snow. I. Observed quantum yield, domain of photolysis, and secondary chemistry. *J. Chem. Phys*., 140, 244305, doi:10.1063/1.4882898, 2014.

Michoud, V., Doussin, Jean-Francois, Colomb, A., Afif, C., Borbon, A., Camredon, M., Aumont, B., Legrand, M., Beekman, M.: Strong HONO formation in a suburban site during snowy days. *Atmos. Environ*., 116, 155-158, doi:10.1016/j.atmosenv.2015.06.040, 2015.

Morin, S., Savarino, J., Frey, M.M., Domine, F., Jacobi, H.-W., Kaleschke, L., Martins, J.M.F.: Comprehensive isotopic composition of atmospheric nitrate in the Atlantic Ocean boundary layer from 65°S to 79°N. *J. Geophys. Res*., 114, D05303, doi:10.1029/208JD010696, 2009.

Oltmans, S.J., Schnell, R.C., Johnson, B.J., Petron, G., Mefford, T., Neely III, R.: Anatomy of wintertime O3 production associated with oil and gas extraction activity in Wyoming and Utah. *Elem. Sci. Anth*., 2, 000024, doi:10.12952/journal.elementa.000024, 2014.

Quinn, P.K., Coffman, D.J., Kapustin, V.N., Bates, T.S., Covert, D.S.: Aerosol optical properties in the MBL during ACE-1 and the underlying chemical and physical aerosol properties. J. Geophys. Res., 103, 16547-16564, 1998.

Quinn, P.K., Bates, T.S., Miller, T.L., Coffman, D.J., Johnson, J.E., Harris, J.M., Ogren, A., Forbes, G., Anderson, T.L., Covert, D.S., Rood, M.J.: Surface submicron aerosol

Maria Zatko 8/10/16 7:44 AM
Deleted: a

chemical composition: what fraction is not sulfate? *J. Geophys. Res*., 105(D5), 6785-6805, doi:10.1029/1999JD901034, 2000.

Rappengluck, B., Ackermann, L., Alvarez, S., Golovko, J., Buhr, M., Field, R.A., Soltis, J., Montague, D.C., Hauze, B., Adamson, S., Risch, D., Wilkerson, G., Bush, D., Stoekenius, T., Keslar, C.: Strong wintertime O3 events in the Upper Green River basin, Wyoming. *Atmos. Chem. Phys*., 14, 4909-4934, doi.10.5194/acp-14-4909-2014, 2014.

Rolph, G.D.: Real-time Environmental Applications and Display sYstem (READY) Website (http://www.ready.noaa.gov). NOAA Air Resources Laboratory, College Park, MD, 2016.

Schnell, R.C., Oltmans, S.J., Neely, R.R., Endres, M.S., Molenar, J.V., White, A.B.: Rapid photochemical production of O3 at high concentrations in a rural site during winter. *Nat. Geosci*., 2, 120-122, doi:10.1038/ngeo415, 2009.

Sigman, D.M., Casciotti, K.L., Andreani, M., Barford, C., Galanter, M., Bohlke, J.K.: A bacterial method for the nitrogen isotopic analysis of nitrate in seawater and freshwater. *Anal. Chem*., 73, 4145-4153, doi:10.1021/ac010088e, 2001.

Silva, S.R., Kendall, C., Wilkinson, D.H., Ziegler, A.C., Chang, C.C.Y., Avanzino, R.J.: A new method for collection of nitrate from fresh water and analysis of the nitrogen and oxygen isotope ratios. *J. Hydrol*., 228, 22-36, 2000.

Stamnes, K., Tsay, S., Wiscombe, W., Jayaweera, K.: Numerically stable algorithm for discrete-ordinate-method radiative transfer in multiple scattering and emitting layered media. *Appl. Opt*., 27, 2502-2509, 1988.

Stein, A.F., Draxler, R.R, Rolph, G.D., Stunder, B.J.B., Cohen, M.D., and Ngan, F.:. NOAA's HYSPLIT atmospheric transport and dispersion modeling system, *Bull. Amer. Meteor. Soc*., 96, 2059-2077, 2015, http://dx.doi.org/10.1175/BAMS-D-14-00110.1

Thompson, A.M., The oxidizing capacity of the Earth's atmosphere: Probable past and future changes. *Science*, 256, 1157-1165, 1992.

US EIA (US Energy Information Administration): Annual energy outlook 2014 Early Release Overview, Office of Integrated and International Energy Analysis US Department of Energy, Washington, DC 20585, available at: http://www.eia.gov/forecasts/aeo/er/pdf/0383er(2014).pdf (last access 24 March 2015), Report, 2014.

Veres, P.R., Roberts, J.M., Wild, R.J., Edwards, P.M., Brown, S.S., Bates, T.S., Quinn, P.K., Johnson, J.E., Zamora, R.J., de Gouw, J.: Peroxynitric acid (HO_2NO_2) measurements during the UBWOS 2013 and 2014 studies using iodide ion chemical ionization mass spectrometry. *Atmos. Chem. Phys*., 15, 8101-8114, doi:10.5194/acp-15-8101-2015, 2015.

Warneke, C., Geiger, F., Edwards, P.M., Dube, W., Petron, G., Kofler, J., Zahn, A., Brown, S.S., Graus, M., Gilman, J.B., Lerner, B.M., Peischl, J., Ryerson, T.B., de Gouw, J.A., Roberts, J.M.: Volatile organic compound emissions from the oil and natural gas industry in the Uintah Basin, Utah: oil and gas well pad emissions compared to ambient air composition. *Atmos. Chem. Phys*., 14, 10977-10988, doi:10.5194/acp-14-10977-2014, 2014.

Warren, S.G., Brandt, R.E., Grenfell, T.C.: Visible and near-ultraviolet absorption spectrum of ice from transmission of solar radiation into snow. *Appl. Opt*., 45, 21, 2006.

Walters, W.W., Goodwin, S.R., Michalski, G.: Nitrogen stable isotope composition $\delta^{15}N$ of vehicle-emitted NO_x. *Environ. Sci. Tech*., 49, 2278-2285, doi:10.1021/es505580v, 2015.

Walters, W.W., Michalski, G.:Theoretical calculation of nitrogen isotope equilibrium exchange fractionation factors for various NO_y molecules. *Geochem. Cosmochem. Acta*., 164, 284-297, doi:10.1016/j.gca.2015.05.029, 2015.

Walters, W.W., Simonini, D.S., Michalski, G.: Nitrogen isotope exchange between NO and NO_2 and its implications for $\delta^{15}N$ variations in tropospheric NO_x and atmospheric nitrate. *Geophys. Res. Lett*., 43, 1, 440-448, 10.1002/2015Gl066438, 2016.

Wild, R.J., Edwards, P.M., Bates, T.S., Cohen, R.C., deGouw, J.A., Dube, W.P., Gilman, J.B., Holloway, J., Kercher, J., Koss, A.R., Lee, L., Lerner, B.M., McLaren, R., Quinn, P.K., Roberts, J.M., Stutz, J., Thornton, J.A., Veres, P.R., Warneke, C., Williams, E., Young, C.J., Yuan, B., Zarzana, K.J., Brown, S.S.: Reactive nitrogen partitioning and its relationship to winter ozone events in Utah. *Atmos. Chem. Phys*., 16, 573-583, doi:10.5194/acp-16-573-2016, 2016.

Wiscombe, W.J.: The delta-M method: Rapid yet accurate radiative flux calculations for strongly asymmetric phase functions. *J. Atmos. Sci*., 34, 1408-1422, 1977.

Yuan, B., Liggio, J., Wentzell, J., Li, S. M., Stark, H., Roberts, J. M., Gilman, J., Lerner, B., Warneke, C., Li, R., Leithead, A., Osthoff, H. D., Wild, R., Brown, S. S., and de Gouw, J. A.: Secondary formation of nitrated phenols: insights from observations during the Uintah Basin Winter Ozone Study (UBWOS) 2014, *Atmos. Chem. Phys*., 16, 2139-2153, 10.5194/acpd-16-2139-2016, 2016.

Zatko, M.C., Grenfell, T.C., Alexander, B., Doherty, S.J., Thomas, J.L., Yang, X., The influence of snow grain size and impurities on the vertical profiles of actinic flux and associated NOx emissions on the Antarctic and Greenland ice sheets. *Atmos*. *Chem*. *Phys*., 13, 3547-3567, doi:10.5194/acp-13-3547-2013, 2013.

Zatko, M.C. and Warren, S.G.: East Antarctic sea ice in spring: spectral albedo of snow, nilas, frost flowers, and slush; and light-absorbing impurities in snow. *Ann. Glaciol.*

Special Issue: Sea ice in a changing environment, 56(69), doi:10.3189/2015AoG69A574, 2015.

Zatko, M.C., Geng, L., Alexander, B., Sofen, E., Klein, K.: The impact of snow nitrate photolysis on boundary layer chemistry and the recycling and redistribution of reactive nitrogen across Antarctica and Greenland in a global chemical transport model. *Atmos. Chem. Phys*., 16, 2819-2842, doi:10.5194/acp-16-2819-2016, 2016.

Zhou, X., Beine, H.J., Honrath, R.E., Fuentes, J.D., Simpson, W., Shepson, P.B., Bottenheim, J.W.: Snowpack photochemical production of HONO: a major source of OH in the Arctic boundary layer in springtime. *Geophys. Res. Lett*., 28(21), 4087-4090, 2001.

Zhu, C., Xiang, B., Chu, L.T., Zhu, L.: 308 nm Photolysis of Nitric Acid in the Gas Phase, on Aluminum Surfaces, and on Ice Films. *J. Phys. Chem. A*., 114, 2561-2568, doi: 10.1021/jp909867a, 2010.

Table 1. Snow photic zone depth and daily-averaged modeled F_{Nr} calculated using E8 and the TRANSITS model on January 22, January 31, and February 4.

Pit Date	Photic zone depth (cm)	Daily-averaged F_{Nr} (molec cm^{-2} s^{-1})		
		E8	TRANSITS (ϕ = 4.6 x 10^{-3})	TRANSITS (ϕ = 0.2)
January 22	5.0	$5.6x10^{8}$	$6.3x10^{8}$	$2.9x10^{10}$
January 31	7.0	$1.9x10^{8}$	$5.6x10^{7}$	$2.7x10^{9}$
February 4	7.0	$3.2x10^{8}$	$1.2x10^{8}$	$5.6x10^{9}$

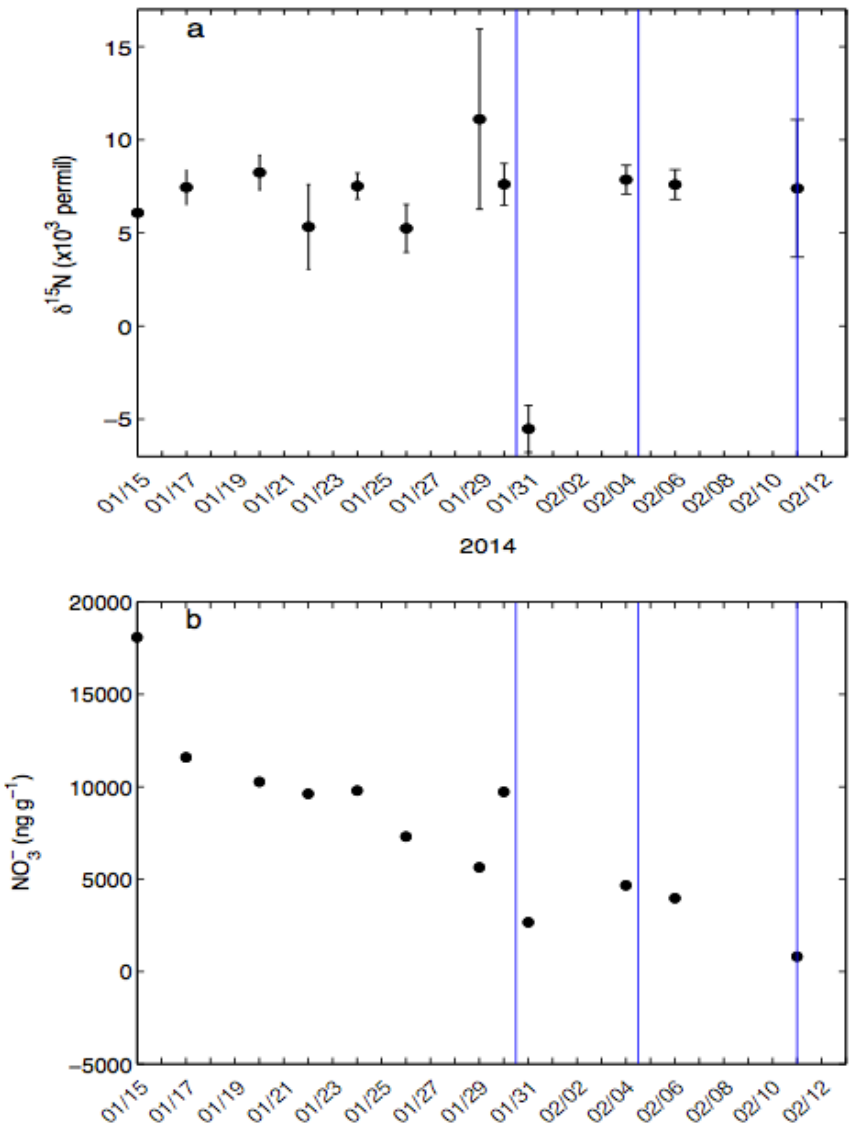

Figure 1. (a) Mean surface snow (top 1 cm) $\delta^{15}N(NO_3^-)$ observations (‰) for triplicate measurements from each snowpit (close circles). The full range of triplicate measured surface snow $\delta^{15}N(NO_3^-)$ for each snowpit is also indicated (vertical black lines). (b) Surface snow nitrate concentration measurements (ng g^{-1}) for each snowpit. The uncertainty in the concentration measurements is 0.75‰. The vertical blue lines indicate snowfall events.

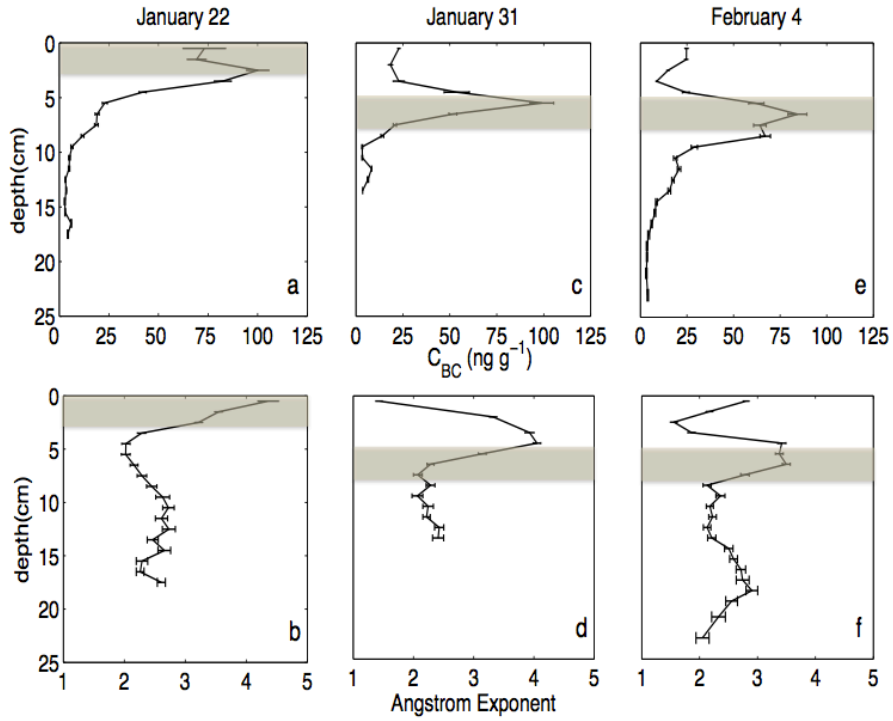

Figure 2. Snow optical properties measured on January 22 (top), January 31 (middle), and February 4 (bottom). (top) Vertical profiles of mean snow black carbon (C_{BC}, ng g^{-1}) measurements and the full range of C_{BC} measured at each depth (horizontal black lines), (bottom) mean Ångstrom exponent (Å, unitless) measurements and the full range of Å measured at each depth (horizontal black lines). The brown shaded region represents the dusty layer as defined in the text.

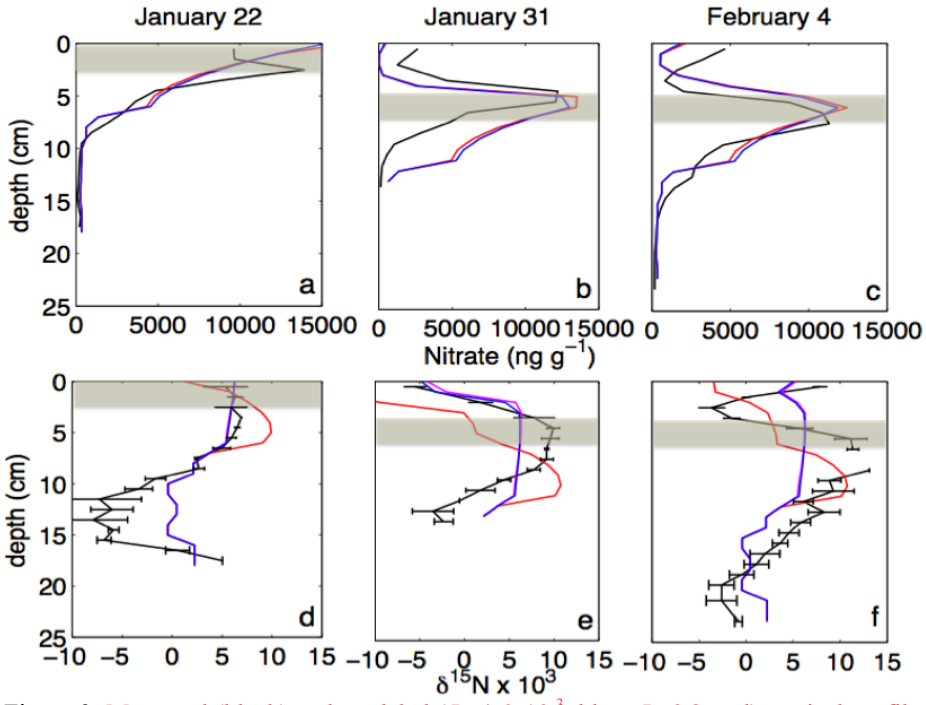

Figure 3. Measured (black) and modeled (Φ=4.6x10^{-3}, blue; Φ=0.2, red) vertical profiles of snow nitrate concentration (top) and $\delta^{15}N(NO_3^-)$ (bottom) on January 22 (left), January 31 (center), and February 4 (right). Modeled $\delta^{15}N(NO_3^-)$ profiles are calculated using variable quantum yields (Φ=4.6x10^{-3}, blue; Φ=0.2, red, Φ=0, magenta). The brown shaded region represents the dusty layer.

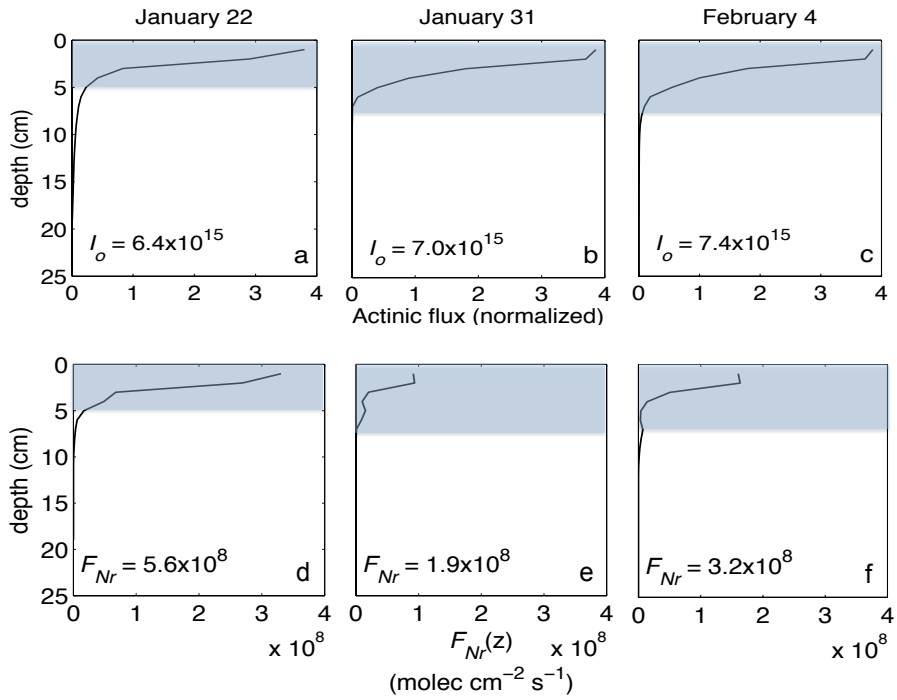

Figure 4. (a-c) Modeled vertical profiles of UV actinic flux (I, photons cm^{-2} s^{-1}) normalized to surface downwelling irradiance (I_o, photons cm^{-2} s^{-1}). Also presented is measured total UV I_o (λ=300-350 nm) for a solar zenith angle of 60° on each day. (bottom) (d-f) Modeled vertical profiles of snow-sourced N_r fluxes (F_{Nr}, molec cm^{-2} s^{-1}) calculated using E8. Also shown is total F_{Nr}, which is the depth-integrated F_{Nr} over the photic zone. The blue shaded region represents the snow photic zone.

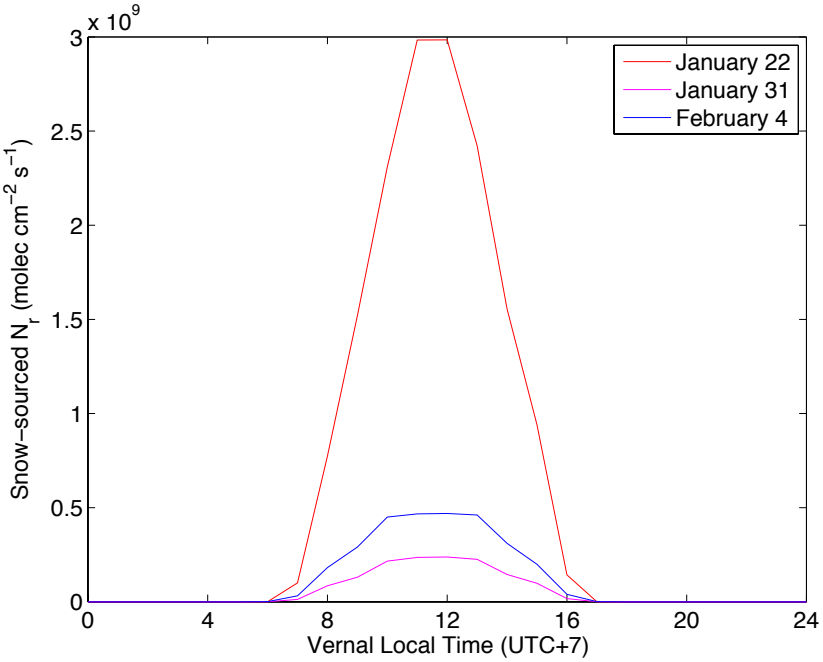

Figure 5. Modeled diurnal profiles of snow-sourced N_r fluxes (F_{Nr}, molec cm^{-2} s^{-1}) calculated using TRANSITS on January 22 (red), January 31 (magenta), and February 4 (blue).

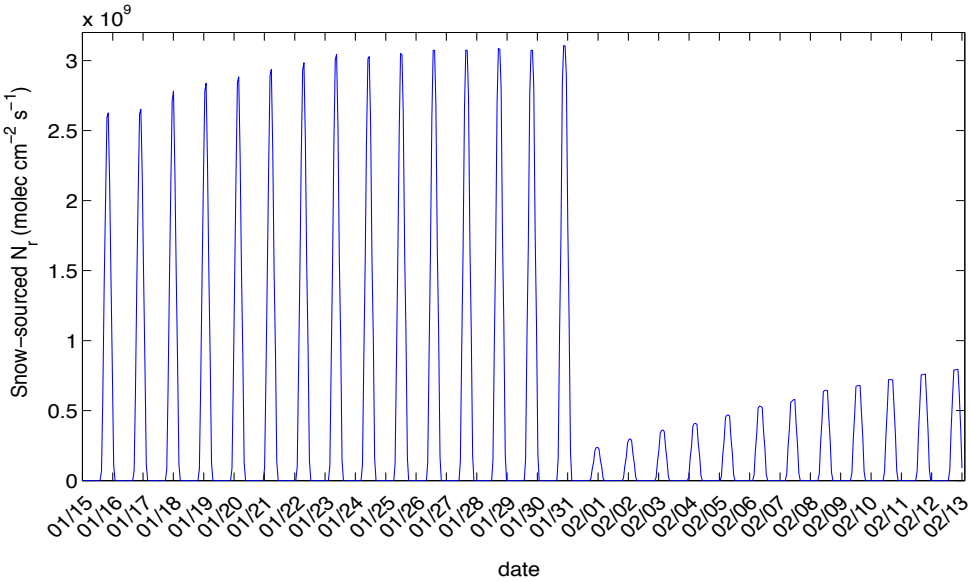

Figure 6: Modeled snow-sourced N_r fluxes (molec cm^{-2} s^{-1}) for each hour during the campaign from January 15 to February 11.